The Journal of Physiology

Dynamics of cardio-muscular networks in exercise and fatigue

Sergi Garcia-Retortillo[1,2] and Plamen Ch Ivanov[3,4]

[1]*Department of Health and Exercise Science, Wake Forest University, Winston-Salem, North Carolina, USA*
[2]*Complex Systems in Sport, INEFC University of Barcelona, Barcelona, Spain*
[3]*Keck Laboratory for Network Physiology, Department of Physics, Boston University, Boston, Massachusetts, USA*
[4]*Institute of Biophysics and Biomedical Engineering, Bulgarian Academy of Sciences, Sofia, Bulgaria*

Handling Editors: Vaughan Macefield & Yoshihiro Kubo

The peer review history is available in the Supporting Information section of this article (https://doi.org/10.1113/JP286963#support-information-section).

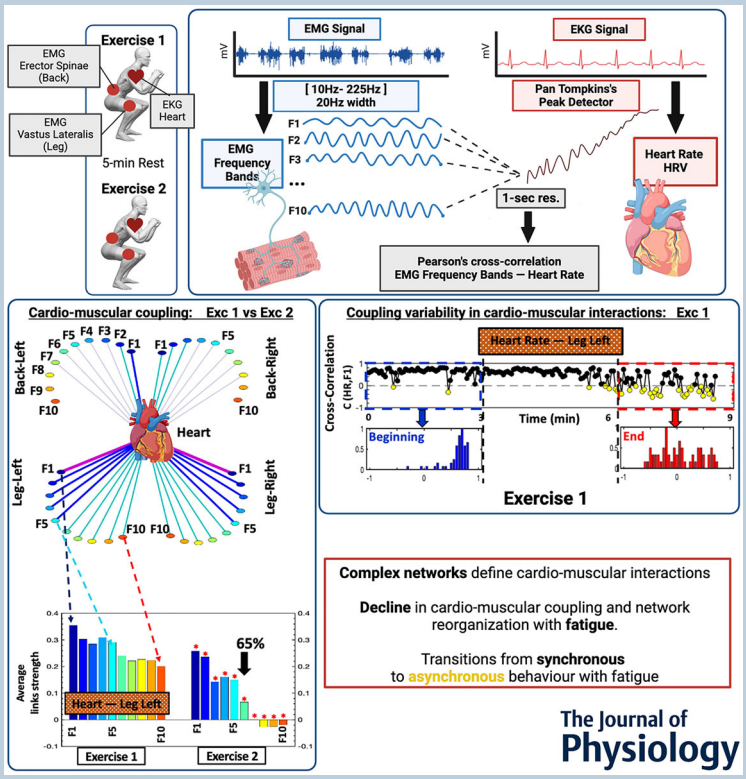

Abstract figure legend This study introduces a pioneering approach to assess cardio-muscular network interactions by examining the synchronization of cardiac function with muscle activity during exercise and fatigue. Participants performed two sets of bodyweight squats until exhaustion, with a 5 min rest period between sets. During the protocol, electrocardiogram (EKG) signals were recorded alongside electromyography (EMG) signals from the left and right vastus lateralis (Leg Left, Leg Right) and erector spinae (Back Left, Back Right) muscles. We decomposed EMG signals into 10 frequency bands (F1–F10) and then cross-correlated these bands with heart rate derived from the EKG. We uncover the first profiles of cardio-muscular interactions characterized by specific hierarchical organization of link strength. We observed a significant decline in the degree of cardio-muscular coupling with fatigue (~65%), marked by complex transitions from synchronous to asynchronous behaviour.

 DOI: 10.1113/JP286963

Abstract A fundamental question in cardiovascular and muscle physiology is how the heart operates in synchrony with distinct muscles to regulate homeostasis, enable movement and adapt to exercise demands and fatigue. Here we investigate how autonomic regulation of cardiac function synchronizes and integrates as a network with the activity of distinct muscles during exercise. Further, we establish how the network of cardio-muscular interactions reorganizes with fatigue. Thirty healthy young adults performed two body weight squat tests until exhaustion. Simultaneous recordings were taken of a 3-lead electrocardiogram (EKG) along with electromyography (EMG) signals from the left and right vastus lateralis, and left and right erector spinae. We first obtained instantaneous heart rate (HR) derived from the EKG signal and decomposed the EMG recordings in 10 frequency bands (F1–F10). We next quantified pair-wise coupling (cross-correlation) between the time series for HR and all EMG spectral power frequency bands in each leg and back muscle. We uncovered the first profiles of cardio-muscular network interactions, which depend on the role muscles play during exercise and muscle fibre histochemical characteristics. Additionally, we observed a significant decline in the degree of cardio-muscular coupling with fatigue, characterized by complex transitions from synchronous to asynchronous behaviour across a range of timescales. The network approach we utilized introduces new avenues for the development of novel network-based markers, with the potential to characterize multilevel cardio-muscular interactions to assess global health, levels of fatigue, fitness status or the effectiveness of cardiovascular and muscle injury rehabilitation programmes.

(Received 19 May 2024; accepted after revision 23 September 2024; first published online 12 October 2024)
Corresponding author P. Ch. Ivanov: Department of Physics, Boston University, 590 Commonwealth Avenue, Boston, MA 02215, USA. Email: plamen@buphy.bu.edu

Key points

- The heart operates in synchrony with muscles to regulate homeostasis, enable movement, and adapt to exercise demands and fatigue. However, the precise mechanisms regulating cardio-muscular coupling remain unknown.
- This study introduces a pioneering approach to assess cardio-muscular network interactions by examining the synchronization of cardiac function with muscle activity during exercise and fatigue.
- We uncover the first profiles of cardio-muscular interactions characterized by specific hierarchical organization of link strength.
- We observe a significant decline in the degree of cardio-muscular coupling with fatigue, marked by complex transitions from synchronous to asynchronous behaviour.
- This network approach offers new network-based markers to characterize multilevel cardio-muscular interactions to assess global health, levels of fatigue, fitness status or the effectiveness of cardiovascular and muscle injury rehabilitation programmes.

Sergi Garcia-Retortillo received his BSc in Exercise Science from the University of Barcelona and a BSc in Physical Therapy from the University of Ramon Llull, Spain. He also holds an MSc in Physical Activity and Health and a PhD in Exercise Science from the University of Barcelona. He is currently serving as an Assistant Teaching Professor in the Department of Health and Exercise Science at Wake Forest University, USA. **Plamen Ch. Ivanov**, PhD, DSc, is the Director of the Keck Laboratory for Network Physiology at Boston University. He has introduced innovative ways to analyse and model physiological systems, adapting and developing concepts and methods from modern statistical physics, nonlinear dynamics and networks theory. Professor Ivanov has pioneered the study of dynamic network interactions of physiological and organ systems. He is the originator and founder of the interdisciplinary field of network physiology.


Introduction

A fundamental question in cardiovascular and muscle physiology is how the heart operates in synchrony with distinct muscles to maintain homeostasis, facilitate movement and adapt to exercise demands and fatigue. The utilization of reductionist approaches has led to great advances in the understanding of the autonomic regulation of the heart, as well as basic muscle physiology at the cellular and molecular levels, with a focus on the microscopic scale of individual muscles. However, the precise mechanisms regulating cardio-muscular coupling remain unknown. Specifically, we do not know the functional forms and physiological principles of dynamic coupling and network communication between the heart and distinct muscle fibre types across muscles, and how these network interactions adapt to exercise and fatigue.

Studies in recent years have investigated the relationship between cardiovascular and locomotor function during exercise (Constantini et al., 2018; Kirby et al., 1989; Niizeki et al., 1993; Nomura et al., 2003). According to this phenomenon, heart rate (HR) and step rate (i.e. number of steps/units of time) naturally align during rhythmic locomotion, maintaining a constant ratio between the two rates (Phillips & Jin, 2013). Optimal alignment between cardiac and locomotor phase timing, holds the potential to enhance haemodynamic efficiency and cardiovascular function during rhythmic exercise, thereby offering advantages for cardiac health (Kirby et al., 1989; O'Rourke et al., 1993; Wakeham et al., 2023; Walløe & Wesche, 1988). More specifically, it has been shown that synchronizing foot strike (corresponding to muscle contraction and peak intra-muscular pressure) with the diastolic phase of the cardiac cycle, as opposed to the systolic phase, significantly reduces HR during exercise and has beneficial metabolic effects (Constantini et al., 2018; Wakeham et al., 2023).

The studies mentioned above offer valuable insights into the relationship between HR and step rate. However, they do not assess dynamic coupling between the heart and different muscle fibre types across various muscles. Firstly, while these methods utilize a direct cardiac measure (e.g. EKG signal), they lack direct measures of muscle activation, relying instead on accelerometers/force sensors as an indirect indicator of muscle function. For a more precise understanding of how cardiac activity synchronizes with muscle activation, employing direct measures such as surface electromyography (EMG) is essential. EMG detects changes in electric potential across the sarcolemma, reflecting alterations in the muscle's excitation state (Vigotsky et al., 2018). Secondly, it is crucial to acknowledge the skeletal muscle's complex nature, comprising multiple muscle fibres that respond individually and uniquely to various environmental influences (Mccarthy et al., 2019). Therefore, to comprehensively understand cardio-muscular coupling, the assessment of how the heart synchronizes its activation with distinct muscle fibre types within muscles is imperative. Lastly, existing works have not explored the dynamic aspects of cardio-muscular coupling. They focused on separate 'snapshots in time' to assess various physiological outcomes (e.g. cardiac afterload, pulmonary ventilation) based on the phase timing between HR and step rate, and did not measure how direct cardio-muscular coupling evolves in time in response to fatigue. Importantly, cardiac and muscular adaptations continuously evolve in time as a result of soft-assembled states dwelling at different timescales and levels of biological system organization (Ivanov et al., 2009; Vázquez et al., 2016). Earlier studies have identified the presence of long-range power-law correlations in the cardiovascular and muscular systems with invariant behaviour at different timescales, indicating the presence of multiscale mechanisms underlying neural regulation of locomotion (Ashkenazy et al., 2002; Hu et al., 2007; Ivanov et al., 2009; Karasik et al., 2002).

To establish the first building blocks of cardio-muscular coordination, we present here a novel analytical approach to assess the direct coupling between cardiac activity (EKG, heart rate variability (HRV)) and activation of distinct muscles (EMG). Specifically, we analyse the degree of cross-correlation between time series of instantaneous HR and EMG spectral power for different frequency bands (amplitude–amplitude coupling). This method allows us to identify basic physiological principles of direct coupling and network communication between autonomic regulation of cardiac function and distinct muscle fibre types across muscles, and how these network interactions evolve over time, adapting to exercise and fatigue. Notably, this method has been successfully utilized to assess how distinct frequency bands embedded in muscle dynamics synchronize with each other and integrate as a network across muscles during exercise, and to establish how the network of inter-muscular interactions reorganizes with fatigue (Garcia-Retortillo & Ivanov, 2022; Garcia-Retortillo et al., 2023; Garcia-Retortillo et al., 2024).

Our first hypothesis was that the cardio-muscular interactions network would exhibit a specific hierarchical organization of coupling strength, depending on the muscle type (histochemical characteristics) and function (e.g. major, supportive) during exercise. Second, we hypothesized that the degree of cardio-muscular coupling would decrease with fatigue as cardiac sympathetic activation and neuromuscular fatigue increase, and would exhibit differentiated responses depending on muscle function and muscle fibre composition. Last, cardio-muscular profiles of link strength would show similar characteristics and similar responses to fatigue across timescales, reflecting the presence of multiscale

mechanisms underlying cardiovascular and muscular function during exercise.

Accordingly, we investigated how autonomic regulation of cardiac function synchronizes and integrates as a network with the activity of distinct muscles during a squat test performed until exhaustion, and established how the network of cardio-muscular interactions reorganizes with fatigue. We discovered that the cardio-muscular network exhibits a complex hierarchical organization of distinct sub-networks and network modules during the squat movement, which depends on muscle function and muscle fibre composition. Our findings indicate that the network organization dynamically reorganizes in response to fatigue and reveal similar characteristics over a range of timescales. The framework of network physiology (Ivanov, 2021; Ivanov & Bartsch, 2014; Lin et al., 2020) and, more specifically, network physiology of exercise (Balagué et al., 2020; Balagué, Garcia-Retortillo, et al., 2022; Balagué, Hristovski, et al., 2022), that we utilize in this study introduces new avenues for the development of novel network-based markers, with the potential to characterize cardio-muscular, inter-muscular and inter-organ network interactions during exercise, assess levels of fatigue, fitness status, or the effectiveness of cardiovascular and muscle injury rehabilitation programmes.

Methods

Ethical approval

The experimental protocol was approved by the local ethical committee (Wake Forest University IRB00024843) and was carried out according to the *Declaration of Helsinki*. Before taking part in the study, participants read the study description and risks and gave informed consent in writing. All ethical regulations were followed.

Participants

To determine the sample size for this study, a power analysis was conducted using G-Power 3.1 (Faul et al., 2007). Previous studies assessing fatigue effects on repeated exercise performed until exhaustion (same research design; 1 group, 2−3 repeated measures) have reported large effect sizes (0.7 and higher (Garcia-Retortillo et al., 2017)). Thus, using an effect size of 0.7, $\alpha < 0.05$, power $(1 - \beta) = 0.90$, we estimated a minimum sample size = 20. Thirty healthy young adults (19 females and 11 males; age 21.27 ± 3.14 years, height 170.62 ± 10.09 cm and mean body mass 65.88 ± 8.34 kg) were recruited for this study. Participants were strictly recruited according to the following inclusion criteria: (a) aged 18−30 years; (b) body mass index (in kg/m^2) >18.5 and <30; (c) normal physical activity >5 and <10 h/week, but without sport specialization (not active athletes); and (d) blood pressure <140/90 mmHg. The following exclusion criteria were applied: (a) intake of prescribed drugs that could negatively affect muscle strength, such as corticosteroids; (b) no current or previous injury that could prevent performance during the experimental protocol test; and (c) any other physical condition (cardiac, respiratory, etc.) that might have prevented the performance of a test protocol involving squat exercise until exhaustion.

Study design and experimental protocol

After the participants gave their signed consent, they made a single visit to the laboratory. Initially, participants familiarized themselves with the squat movement, practising until they could execute it according to the provided protocol instructions (see below). Following a 5 min rest, participants engaged in the study's test protocol, which included two sets of squats performed until exhaustion (Exercise 1 and Exercise 2), separated by 5 min rest intervals. The squat sets were conducted according to the following instructions: (i) feet positioned slightly wider than shoulder-width apart; (ii) arms extended straight out; (iii) initiating the movement by inhaling and unlocking the hips, gently pushing them backwards; (iv) continuing to move hips backwards as the knees began to flex; (v) squatting down until reaching a guiding rope designed to ensure a consistent range of motion (further details below); (vi) returning to a standing position; and (vii) repeating the squat movement until exhaustion. The guiding rope was set at a height corresponding to the level of participants' thighs at the squat's bottom position when their thighs were parallel to the ground. Participants were instructed to maintain an upright chest, keep their weight over their heels and prevent their knees from moving inward (Bianco et al., 2015).

The back squat variation was chosen for the exercise protocol in this study because it is more commonly used in training and daily activities than the front squat variation (Yavuz et al., 2015). Additionally, the back squat was preferred as it requires less ankle mobility, considering that limited ankle dorsiflexion is a common characteristic in the general population (Rabin & Kozol, 2017). The tempo of the squatting movements was regulated by a metronome (MetroTimer version 3.3.2, ONYX Apps), employing a 3:3 rhythm, consisting of 3 s for the downward movement and 3 s for the upward movement, making each squat last for a total of 6 s. In our protocol, squat movements during each exercise segment continued until participants were unable to perform the next squat or maintain the required 3:3 squat tempo.

The repetition of two consecutive exercise bouts until exhaustion, with a 5 min rest in between, allowed us

to observe the effects of acute fatigue (the accumulation of fatigue within exercise segments) and residual fatigue between Exercise 1 and Exercise 2. Acute fatigue arises when energy consumption surpasses the muscle's aerobic capacity, requiring a substantial portion of energy to come from anaerobic metabolism. In contrast, residual fatigue encompasses neuromechanical and biochemical alterations (such as a decrease in maximal force) induced by prior exercise (i.e. Exercise 1) (Hader et al., 2019).

Three markers were utilized to assess the levels of fatigue and global physiological function during the experimental protocol: (i) changes in HR and heart rate variability (HRV; (ii) changes in the amplitude of the EMG signal; and (iii) test performance, measured as the number of squats participants performed during Exercises 1 and 2.

Electrocardiography and electromyography acquisition and signal processing

Participants were asked to wear appropriate clothing that would not obstruct EKG and EMG electrode placement sites. Before the mounting of the EKG and EMG electrodes, participants' skin was shaved and cleaned using alcohol and left to dry for 60 s to reduce the myoelectrical impedance, according to the SENIAM guidelines (Hermens et al., 2000). A small amount of skin prep gel was also used to enhance the signal quality (Nuprep, Weaver and Company, USA). A standard 3-lead EKG set-up was used to obtain the recording for lead II during the entire protocol: right shoulder (−), left shoulder (ground) and lower left abdomen (+). EMG signals were also recorded simultaneously with the EKG signal from the following muscles: left and right vastus lateralis (Leg-Left and Leg-Right muscles); left and right erector spinae longissimus (Back-Left and Back-Right lower back muscles). The exact location of the surface electrodes' (Meditrace Foam EG200, Danlee Medical Products Inc., Syracuse, USA) placement on each muscle was carried out according to the recommendations of the SENIAM organization. More specifically, vastus lateralis electrodes were placed two thirds of the way along the line from the anterior spina iliaca superior to the lateral side of the patella, and the erector spinae electrodes were located a two-finger width lateral from the spinous process of vertebra L1 (Fig. 1*A & B*). The aforementioned Leg and Back muscles were selected because they present the highest myoelectrical activity during bodyweight squat movement (Khaiyat & Norris, 2018). After the electrodes were secured with tape to minimize movement artefacts, a signal quality check was performed to ensure EKG and EMG signal validity.

A Biopac MP150 unit (Biopac Systems Inc, Goleta, CA, USA) was used to collect synchronized EKG (BN-RSPEC2-T) and EMG (BN-EMG2-T) signals. Data were processed by means of Matlab (Mathworks, Natick, MA, USA). EKG and EMG raw data were recorded at a sample frequency of 2000 Hz and filtered using a 0.5–150 Hz (EKG) and 5−500 Hz (EMG) bandpass filter. A Notch filter was used with a width of 1 Hz at the frequency of 60 Hz to remove line interference from the grid for both EKG and EMG signals.

Note that in this study we employed a similar method to assess and quantify cardio-muscular interactions as in previous works (Garcia-Retortillo & Ivanov, 2022; Garcia-Retortillo et al., 2023; Garcia-Retortillo et al., 2024): (i) spectral decomposition, (ii) cross-correlations between time series of spectral power, (iii) Fourier phase randomization surrogate test, as well as (iv) a same data visualization method (cardio-muscular interaction networks and corresponding bar plots; see below). To investigate the temporal variability in cardio-muscular coupling between HR and EMG spectral power frequency bands that occur as a result of synchronous modulation of their amplitudes at short timescales of a few seconds, here we added additional steps (see *Global measures of cardio-muscular coupling at large timescales*).

Instantaneous heart rate time series

Heartbeat detection in EKG signals is based on the nearly periodic occurrence of R waves (Christov, 2004). To detect R waves in the EKG we apply the Pan–Tompkins algorithm (Pan & Tompkins, 1985). The algorithm consists of the following steps: bandpass filtering, differentiation, squaring of samples, smoothing with a moving average filter, correlation analysis and thresholding (Sieciński et al., 2020). To obtain the instantaneous HR we take the inverse of the resulting R–R intervals and multiply the result by 60.

Next, we perform cubic spline interpolation to generate a new HR time series with a 1 s resolution. We adopt this approach to align the resolution with that of the EMG frequency bands time series (see *Instantaneous heart rate time series*). The obtained HR time series was then normalized to zero mean ($\mu = 0$) and unit standard deviation ($\sigma = 1$).

To remove artefacts from the HR recordings, we implemented the following procedure: at each data point, if the HR value exceeded or fell below two times the standard deviation of the average HR calculated within a 10 s window, the HR value was replaced with the average value for that specific window.

Spectral decomposition of EMG signals: EMG frequency bands time series

We first segmented the EMG signals from the left and right vastus lateralis (Leg-Left and Leg-Right muscles) and the left and right erector spinae longissimus (Back-Left and Back-Right) into 2 s time windows with 1 s over-

lap across Exercise 1 and Exercise 2. Within each 2 s time window, we extracted the spectral power S(f) from each EMG signal using the 'pwelch' function in Matlab, based on the discrete Fourier transform and the Welch's overlapped segment averaging estimator. For each time window we obtained a spectral power value in bins of 0.5 Hz for the range [5–250 Hz], that is, $N = 490$ is the number of spectral power data points for each window of 2 s. To probe specific contributions from different frequency bands F_i to the spectral power within each 2 s time window of the EMG signal, we considered 10 frequency bands with an equal width of 19.5 Hz. To select the range and width of the frequency bands, we referred to previous work investigating the spectral power profiles of the vastus lateralis and erector spinae muscles during the squat exercise (Garcia-Retortillo et al., 2020). The frequency range of 10–230 Hz was chosen because skeletal muscles typically show activity in the spectral power distribution within this frequency range during exercise. A specific bandwidth of 19.5 Hz was selected to obtain detailed profiles of cardio-muscular coordination. Notably, Garcia-Retortillo et al. (2020) demonstrated that the 10−20 Hz bandwidth provides detailed information on the specific contributions of distinct frequency bands within the spectral distribution of muscle activity during exercise. These frequency bands may reflect the range of activity of different types of muscle fibres in each Leg and Back muscle, i.e. F1 = [10–29.5 Hz], F2 = [30–49.5 Hz], F3 = [65–84.5 Hz], F4 = [85–104.5 Hz], F5 = [105–124.5 Hz], F6 = [125–144.5 Hz], F7 = [145–164.5 Hz], F8 = [165–184.5 Hz], F9 = [185–204.5] and F10 = [205–224.5 Hz].

We next calculated the sum of the power $\tilde{S}(f)$ across all frequency bins within each frequency band: $\tilde{S}(f) := \sum_{i=1}^{n} S(f_i)$, where f_i are all $n = 39$ frequencies considered in each frequency band F_i. Thus, we obtained 10 time series of EMG band power $\tilde{S}(f)$ with 1 s resolution for each muscle during the two exercise sets, representing the dynamics of all representative EMG frequency bands. Frequencies below 40−60 Hz (corresponding to our frequency bands F1 and F2) may be attributed to the activity of small alpha-motor neurons that innervate type I slow muscle fibres. The frequency range 60−120 Hz (bands F3–F7) could be attributed to medium alpha-motor neurons that innervate type IIa intermediate (oxidative) fibres, and high frequencies in the range 170−220 Hz (bands F8–F10) may correspond to larger alpha-motor neurons that connect to type IIb fast (glycolytic) fibres (Dreibati et al., 2010; Grimby et al., 1979, 1981; Rosenblum et al., 2021; Wakeling et al., 2001). The [50–65 Hz] range was ignored due to the Notch filter at 60 Hz to remove interference from the electric grid. The obtained 10 times series of EMG spectral power for each band F_i were then normalized to zero mean ($\mu = 0$) and unit standard deviation ($\sigma = 1$). The obtained time series of EMG power $\tilde{S}(f)$ in each frequency band F_i reflected the micro-architecture (in 1 s resolution) of synchronous modulation in the amplitude of muscle activation and allowed variations in coupling and network interactions between EMG frequency bands F_i and instantaneous HR to be tracked.

Global measures of cardio-muscular coupling at large timescales

To investigate cardio-muscular interactions between HR and EMG frequency bands at large timescales of observation, we performed the steps below separately for (i) the Beginning (first third) *vs*. End (last third) segments of Exercise 1 (accumulation of fatigue; Fig. 2); and (ii) Exercise 1 *vs*. Exercise 2 (residual fatigue; Figs 3 and 4). We considered all pairs between the heart and selected muscles (i.e. heart–muscle sub-networks) involved in the squat movement (Heart-LegL; Heart-LegR; Heart-BackL and Heart-BackR).

Cross-correlations between time series of instantaneous heart rate and EMG frequency bands. For each heart–muscle sub-network, we calculated the bivariate equal-time Pearson's cross-correlation between HR and all EMG spectral power $\tilde{S}(f)$ frequency bands F_i where i = 1,…,10. This led to $1 \times 10 = 10$ cross-correlation values C for each heart–muscle pair, as shown in the bar plots in Figs 2*B* and 3*B*. Note that C quantifies the degree of coupling between HR and the EMG frequency band F_i from one muscle. The cross-correlation values ranged from $C = -1$ (fully anti-correlated) to $C = 1$ (fully positively correlated), with $C = 0$ indicating the absence of linear relation between the HR and the power $\tilde{S}(f)$ time series of a given EMG frequency band. When cross-correlating the HR time series with the spectral power time series of one EMG frequency band for an entire exercise bout, we found that the highest coefficient was the one corresponding to zero lag (no delay). Our analyses of entire exercise bouts showed that the larger the delay in the cross-correlation, the lower the cross-correlation coefficient and thus weaker interactions and network links.

Fourier phase randomization surrogate test and significance threshold for link strength in networks of cardio-muscular interactions. To illustrate the physiological relevance of the cardio-muscular interaction networks derived from our empirical analysis, we conducted a Fourier phase randomization surrogate test (Kantz & Schreiber, 2003; Schreiber & Schmitz, 2000; Theiler et al., 1992) on the recorded EMG signals (LegL, LegR, BackL and BackR). This test preserves the overall spectral power in the various frequency

bands F_i within the EMG recordings while eliminating Fourier phase information related to nonlinear EMG characteristics. Consequently, it eliminates disparities in the fine temporal structure associated with short-term modulations in the spectral dynamics of EMG frequency bands F_i within a muscle. It's worth noting that in the Fourier -phase-randomized surrogate EMG signals, the relative ratios among the average spectral power of muscle activation in the frequency bands F_i are retained. Still, synchronous modulations in EMG frequency bands that contribute to effective cross-frequency coupling and capture the nonlinear features of EMG signals were removed. As a result, the degree of coupling between the instantaneous HR and the EMG frequency bands F_i from different muscles is remarkably reduced after the Fourier phase randomization procedure, since physiologically relevant information regarding coordinated activation of distinct frequency bands is lost.

Moreover, to assess the statistical significance and physiological relevance of the observed hierarchical network organization and its changes with fatigue, we introduced an additional step in our surrogate test to determine the significance threshold for network link strength. Specifically, for each network link, we generated surrogates considering signals from every possible pair of randomly chosen subjects. Since we have 30 subjects in the database, 435 pairs of random subject combinations were generated. Each heart–muscle pair (Heart-LegL, Heart-LegR, Heart-BackL and Heart-BackR) involves 10 links between the HR and the 10 frequency bands F_i of the corresponding muscle in the pair. Thus, combining the four sub-networks representing all heart–muscle pairs we obtained a distribution of 17,400 surrogate links (cross-correlation values) for Exercise 1 and Exercise 2 – i.e. 4 heart–muscle pairs $\times$ 10 links $\times$ 435 subject combinations $=$ 17,400 surrogate links. For each protocol segment distribution, the mean μ_{surr} and standard deviation σ_{surr} were obtained. Thus, the significance threshold for Exercise 1 and Exercise 2 at a 95% confidence level for the network link strength was defined as $\mu_{surr} + 2\sigma_{surr}$. We found that the significance threshold for network link strength was $Th_{exercise} = 0.1$ (corresponding to the highest Th value during the exercise segments).

Network maps of cardio-muscular interactions. A multiplex network of sub-networks was obtained to visualize interactions from all heart–muscle pairs and their hierarchical organization within the network (Figs 2*A* and 3*A*). We mapped the results of our cross-correlation analyses (section Spectral decomposition of EMG signals) into different group-averaged networks for the Beginning (first third) and End (last third) segments during Exercise 1 (Fig. 2*A*; accumulation of fatigue), and across Exercise 1 and Exercise 2 (Fig. 3*A*; residual fatigue). The graphical approach we employed is essential to identify universal patterns in the cardio-muscular network structure, the hierarchical organization of sub-networks and modules, and to track the transition in network characteristics with accumulation of fatigue. Each muscle is represented by a semicircle where colour nodes represent distinct frequency bands F_i that could correspond to activation of different muscle fibre types in the muscle (see *Instantaneous heart rate time series*, Methods). Network links correspond to the cross-correlation values C obtained from the cross-correlation analysis (section Spectral decomposition of EMG signals) and reflect the coupling strength between HR and a given frequency band from the muscle in the heart–muscle sub-network. Link strength is marked by line colour and width – we use a distinct link colour code to demonstrate network reorganization with fatigue. To represent how network organization changes with the accumulation of fatigue during Exercise 1 (Fig. 2*A*) and with residual fatigue across repeated exercise bouts (Exercise 1 and Exercise 2; Fig. 3*A*), we used the following link strength classification: weak links ($0.05 < C_{i,j} < 0.15$; very thin grey lines), intermediate links ($0.15 < C_{i,j} < 0.25$; thin green lines), strong links ($0.25 < C_{i,j} < 0.35$; dark blue thick lines) and very strong links ($C_{i,j} > 0.35$; magenta very thick lines). Links corresponding to cross-correlation values $C_{ij} < 0.05$ are not shown on the network maps.

Temporal variability in cardio-muscular coupling at short timescales

We further investigated the temporal coupling variability between HR and EMG spectral power frequency bands that occur as a result of synchronous modulation of their amplitudes at short timescales of a few seconds (Fig. 6). We performed the steps below separately for (i) the Beginning (first third) *vs.* End (last third) segments of Exercise 1 (accumulation of fatigue; Fig. 7); and (ii) Exercise 1 *vs.* Exercise 2 (residual fatigue; Fig. 8).

Cross-correlations between HR and EMG frequency bands during Exercise 1. We divided the previously obtained HR and EMG frequency bands time series into NL segments of length $=$ 6 s with 3 s overlap ($NL = (N/L)$), where N is the length of the time series. We selected a 6 s length with a 3 s overlap since one squat movement (3 s down and 3 s up) lasted 6 s. Note that in this step we normalized both the HR and EMG frequency band time series to zero mean ($\mu = 0$) and unit standard deviation ($\sigma = 1$) separately for each 6 s segment.

For each heart–muscle sub-network (Heart-LegL, Heart-LegR, Heart-BackL and Heart-BackR) and for

each 6 s segment, we calculated the bivariate equal-time Pearson's cross-correlation between HR and all EMG spectral power $\tilde{S}(f)$ frequency bands F_i where $i = 1,\ldots,10$. This led to $1 \times 10 = 10$ cross-correlation values C for each heart–muscle sub-network and 6 s segment. The cross-correlation values range from $C = -1$ (fully anti-correlated) to $C = 1$ (fully positively correlated), with $C = 0$ indicating the absence of linear relation between the HR and the power $\tilde{S}(f)$ time series of a given EMG frequency band. This approach enabled us to monitor the impact of fatigue on cardio-muscular coupling variability at a 3 s resolution (6 s windows with 3 s overlap), and to track the transition from positive to negative coupling between HR and EMG frequency bands as fatigue levels increase (see Fig. 6).

Coupling profiles and degree of positive- and anti-correlation between HR and EMG frequency bands during Exercise 1. Since we observed complex transitions from synchronous to asynchronous behaviour with fatigue at short timescales of 3 s (Fig. 6), we next characterized the degree of positive- and anti-correlation between the heart and leg/back muscles. For each pair of HR and EMG frequency bands within each heart–muscle sub-network (Heart-LegL, Heart-LegR, Heart-Back and Heart-BackR), we obtained a histogram of cross-correlation distribution profile by dividing the range $[-1, 1]$ of cross-correlation values into bins of size $\Delta c = 0.05$. The histogram was then rescaled by the maximum number of counts. The obtained distribution profile is proportional to the probability density of cardio-muscular coupling between HR and EMG frequency bands that occurs at short timescales of 3 s.

To quantify the probabilities of finding positively ($C > 0$) or negatively $C < 0$) cross-correlated pairs of HR and EMG frequency bands within each heart–muscle sub-network, we estimated the areas under the distribution profile (histograms) that are above or below zero and normalized by the total area under the profile (see schematic diagram in Fig. 7*A*). The degree of coupling between HR and EMG frequency bands for each heart–muscle sub-network is shown as bar plots (Figs 6*B* and 7*A*), where black positive bars represent the degree of positive correlation ($C > 0$), and yellow negative bars represent the degree of anti-correlation ($C < 0$).

We further dissected the cardio-muscular coupling at short timescales of 3 s by constructing two sets of dynamic networks based on positive- and anti-correlations between HR and EMG frequency bands (Figs 6*C* and 7*B*). Each muscle is represented by a semicircle where colour nodes represent distinct frequency bands F_i. Network links correspond to the bar plots in Figs 6*B* and 7*A*, and represent the degree of positive (top panels) or negative (bottom panels) coupling between HR and EMG frequency bands. Links are linearly scaled with thickness and colour (thicker and darker lines represent stronger coupling). The coexistence of both positively and anti-correlated networks demonstrates a complex duality and the transient nature of cardio-muscular coupling.

Statistical tests

Statistical analyses were performed using Matlab (Mathworks, Natick, MA, USA). We found a non-Gaussian distribution for the cardio-muscular coupling values obtained for the individual subjects in our database (see boxplots for the link strength in different network modules presented in Fig. 5). Thus, to assess effects of accumulation of fatigue during Exercise 1 (Beginning *vs*. End segment), and residual fatigue for repeated Exercise 1 and Exercise 2 on average link strength, we utilized non-parametric Wilcoxon's matched-pairs tests (alpha level 0.05). To account for the multiple comparisons in our analysis of coupling strength across multiple frequency bands and muscles, we employed the false discovery rate control using the Benjamini–Hochberg procedure. This method provides a balance between discovering true effects and controlling the proportion of false positives. Specifically, we applied the Benjamini–Hochberg procedure to adjust the P values for our 10 network links within each heart–muscle sub-network, comparing Beginning *vs*. End and Exercise 1 *vs*. Exercise 2.

Results

We identified and characterized the network of cardio-muscular interactions during a squat test performed until exhaustion and assessed how the network structure reorganizes for two repeated sets. We recorded EKG and EMG data from four muscles – left and right vastus lateralis (LegL and LegR), and left and right erector spinae (BackL and BackR).

Periodic components and trends in heart rate and EMG data

We noted that periodic components and trends embedded in the data reflect important aspects of physiological regulation, responses to movement and exercise-induced fatigue. We identified the following dynamic patterns in the EMG and HR signals during exercise (Fig. 1*C & D*): (i) A prominent 6 s periodic component embedded in the original EMG signal as well as in the EMG spectral bands F1–F10. This periodicity relates to the protocol design where subjects squatted following a metronome with movement 3 s down and 3 s up. (ii) A significant trend with

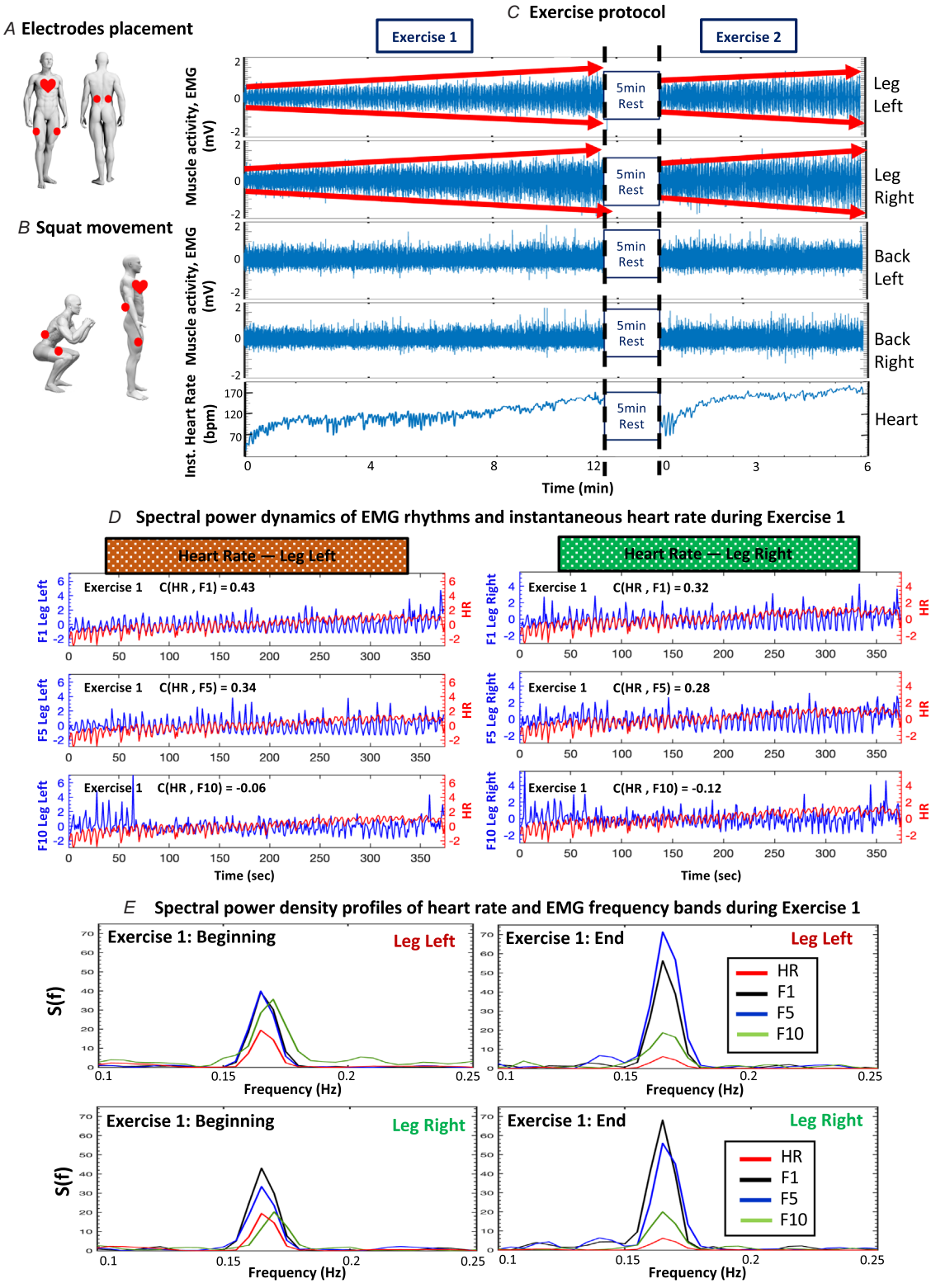

Figure 1. Experimental set-up, dynamics and spectral power of heart rate and muscle activity frequency bands

A, red marks show EKG and EMG electrode placement for simultaneous recording during the squat exercise. EMG is recorded from selected muscles: left and right vastus lateralis (LegL, LegR); left and right erector spinae (BackL, BackR). *B*, schematic representation of squat movement. *C*, dynamics of instantaneous heart rate (HR) and EMG recorded from each muscle – HR and EMG amplitude increase with the accumulation of fatigue during

each exercise bout; higher EMG amplitude at the Beginning of Exercise 2 *vs*. Exercise 1 indicates residual fatigue. Each exercise bout is performed until exhaustion (Methods). *D*, time series of HR (red lines; right vertical axis) and spectral power EMG frequency bands (F1, F5 and F10; blue lines; left vertical axis), show synchronous modulation (data from two representative subjects during Exercise 1). The high degree of synchronous modulation with zero time delay between HR and low-frequency F1 EMG band (LegL and LegR) suggests strong coupling between HR variability and activation of type I slower muscle fibres. Less pronounced synchronization between HR and high-frequency EMG bands F5 and F10 (LegL and LegR) suggests weaker coupling between HR and the activity of type II faster muscle fibres. Synchronization of HR and muscle activity evolves during exercise and is gradually reduced with accumulation of fatigue (Beginning *vs*. End segment of Exercise 1) – an effect observed for all pairs of HR and EMG frequency bands, leading to a reduction of the cross-correlation measure $C(HR,F_i)$. Note that reduction in $C(HR,F_i)$ results from two separate effects: (i) a time shift of peaks (increased time delay) in spectral power related to keeping squat rhythmicity fixed (6 s/squat; see Exercise protocol, Methods) while HR increases with fatigue, and (ii) a loss of the oscillatory activation pattern in HR activity and different EMG frequency bands, transitioning to a more stochastic/noisy behaviour with fatigue. *E*, spectral power density profiles of HR and EMG frequency bands during Exercise 1. Each panel shows the spectral power distribution for HR, F1, F5, and F10 of Leg Left and Leg Right muscles comparing the Beginning (first third; left panels) and End (last third, right panels) of Exercise 1. There is a pronounced stable peak in the spectral power at around 0.15 Hz, reflecting the periodicity corresponding to the squat movements (1 squat/6 s). Notably, this periodic component at 0.15 Hz is present at the Beginning as well as at the End of Exercise 1, despite pronounced trends of increasing spectral power of EMG rhythms and declining HR spectral power with fatigue at the End of exercise.

increasing amplitude of the EMG signal and EMG spectral bands, reflecting an increase in motor unit recruitment with accumulation of fatigue. (iii) A prominent oscillatory pattern in the HR that matches the 6 s periodicity in the EMG signal. This reflects the effect of respiratory cycles on HRV (increase in HR with inspiration and decrease of HR with expiration, i.e. respiratory sinus arrhythmia (RSA)), where respiratory cycles are entrained with the tempo of squat movements. (iv) A trend of non-linear decline in the RSA amplitude in the HR that occurs in response to increasing respiratory rate during exercise to satisfy increased oxygen demands with fatigue (an effect more pronounced at the End of the exercise bout). This behaviour aligns with classical empirical findings by Angelone and Coulter (1964) of how the RSA amplitude changes as a function of breathing frequency. (v) Synchronicity of the HR oscillatory pattern with the 6 s periodic component in the EMG frequency bands, which breaks down to asynchronous (out of phase) behaviour with increasing breathing frequency and fatigue by the End of the exercise (Fig. 1*D*). (vi) Several trends underlying cardiac dynamics related to (a) a gradual increase in HR (Ivanov et al., 1998), (b) a decline in the standard deviation of heartbeat fluctuations (Peng et al., 1995), and (c) a transition in HRV auto-correlations (Karasik et al., 2002) in response to parasympathetic withdrawal and increased sympathetic tone with exercise-induced fatigue.

The observations of prominent periodic components in the time series of EMG spectral bands and HRV throughout the entire exercise bout are validated by systematic analysis of the spectral power of these signals, comparing the Beginning (first third) *vs*. End (last third) of exercise for each individual subject (Fig. 1*E*). Our analyses show there is a pronounced stable peak in the spectral power of EMG and HRV at around 0.15 Hz, reflecting the periodicity corresponding to the squat movements (1 squat/6 s). Notably, this periodic component at 0.15 Hz is present at the Beginning as well as at the End of Exercise 1, despite pronounced trends of increasing spectral power of EMG rhythms (higher peak in S(f)) and declining HR spectral power (lower peak in S(f)) with fatigue at the End of exercise (Fig. 1*E*). This demonstrates that the reported decline in cardio-muscular coupling with fatigue (as measured by the amplitude–amplitude Pearson correlation) is not due to loss of periodicity with fatigue in some of the physiological signals, and rather reflects the loss of coordination/synchrony of the periodic oscillations in HR and EMG frequency bands.

While non-stationarities and trends in the characteristics of physiological signals affect their cross-correlations (Podobnik et al., 2007, 2009), periodic patterns and trends embedded in the data carry very relevant physiological information regarding systems regulation and response to perturbations and fatigue that are reflected by changes in the cross-correlation measure. For this reason, we did not detrend/remove these components from the data.

However, it is important to assess the relative contribution of the periodic components and trends on the cross-correlation measures and derived cardio-muscular physiological networks. We repeated our analysis after detrending the EMG frequency bands and HR signals but preserving the periodic patterns and their amplitude fluctuations (see section *Cardio-muscular networks and reorganization across Exercise 1 and Exercise 2: residual fatigue*).

Further, the experimental data we show in Fig. 1*D* demonstrates the relation between the cross-frequency coupling function and the accumulation of fatigue. In the Beginning segment of Exercise 1, bursts in the instantaneous HR and in the spectral power of (F1) EMG frequency band are well synchronized (synchronous

movement of the red and blue lines in Fig. 1*D*; Top panels). In contrast, the End segment of Exercise 1 exhibits a dramatic decrease in HR variability and an increase in the spectral power amplitude of the (F1) band (indicators of parasympathetic withdrawal and fatigue accumulation), which is notably paralleled by a loss of coordination/synchrony of bursts between HR and the (F1) band (shift of peaks between the red and blue lines in Fig. 1*D*; Top panels). Note the gradual loss of synchrony in bursting activity between HR and higher (F5) and (F10) EMG bands, quantified by a significant decline in the degree of cross-correlation C(HR,F5) and C(HR,F10).

We found that the cardio-muscular network during the squat movement is characterized by an ensemble of interaction sub-networks representing all pairs of heart–muscle (Heart-LegL, Heart-LegR, Heart-BackL and Heart-BackR), where each sub-network exhibits a specific pattern of synchronization (hierarchical structure in network link strength) between instantaneous HR and myoelectrical rhythms associated with different types of muscle fibre. With the accumulation of fatigue within Exercise 1, and with residual fatigue for repeated bouts of Exercises 1 and 2, our results uncovered a complex hierarchical reorganization in the coupling strength where distinct sub-networks within the entire cardio-muscular network respond in a targeted way to overcome the squat test demands. These general observations reflect the complex and dynamic interplay between cardiac autonomic regulation and muscle function during exercise.

Additionally, we quantified exercise performance by measuring the number of squat repetitions. Notably, the number of squats significantly decreased comparing Exercise 1 *vs*. Exercise 2 (62.25 ± 15.61 and 29.26 ± 10.32 in Exercises 1 and 2, respectively; Wilcoxon's test $Z = 2.91$, $P = 0.003$).

Global measures of cardio-muscular coupling at large timescales

To quantify networks of cardio-muscular interactions at large timescales, we mapped the results of our cross-correlation analyses into dynamic networks where nodes correspond to distinct myoelectrical rhythms representing the activity of distinct muscle fibres, and links represent the coupling strength between HR and EMG frequency bands F_i across muscles (Figs 2*A* and 3*A*).

Cardio-muscular networks and reorganization during Exercise 1: accumulation of fatigue. Cardio-muscular interactions between HR and EMG frequency bands from Leg and Back muscles form a multiplex network with pronounced heterogeneity, characterized by distinct topology and hierarchical organization for distinct heart–muscle sub-networks in response to accumulated fatigue (Fig 2*A*). Bar plots in Fig. 2*B* depict link strength profiles for all cardio-muscular interaction sub-networks (Heart-LegL, Hear-LegR, Heart-BackL, Heart-BackR). Each of the 10 bars in the profile represents a link in the corresponding network in Fig. 2*A* and quantifies the coupling strength C(HR,F_i) between HR and the EMG frequency band F_i from one muscle.

At the Beginning of Exercise 1, the link strength profiles for all heart–muscle sub-networks are characterized by stronger coupling between HR and low (F1–F5) EMG frequency bands (i.e. first five bars of the profile), compared with intermediate/fast (F6–F10) EMG bands (i.e. last five bars of the profile). Note that both Heart-Leg (top panels Fig. 2*B*) and Heart-Back sub-networks (bottom panels Fig. 2*B*) show similar link strength profiles, where coupling strength decreases gradually across links from C(HR,F1) to C(HR,F10). However, coupling strength for the Heart-Back sub-networks is slightly weaker than for the Heart-Leg sub-networks.

With the accumulation of fatigue at the End of Exercise 1, a statistically significant decline in coupling strength between HR and EMG frequency bands was observed for all heart–muscle sub-networks. Note that this decline is more pronounced for the coupling between HR and (F1–F5) EMG bands compared with the (F6–F10) bands, leading to a change in the shape of the link strength profiles – from a profile with gradual decline in coupling strength at the Beginning, to a flat profile with similar coupling strength across all links at the End of Exercise 1 (Fig. 2*B*). While both Heart-Leg (Fig. 2*B* top panels) and Heart-Back sub-networks (Fig. 2*B* bottom panels) exhibit the same type of response to accumulated fatigue, the change for the Heart-Back is more pronounced than for the Heart-Leg sub-network (∼55% *vs*. ∼45%, respectively). Red stars in Fig. 2*B* mark statistically significant differences in link strength comparing Beginning *vs*. End of Exercise 1 (Heart-LegL: $P = 0.0004$–0.030; Heart-LegR: $P = 0.0001$–0.016; Heart-BackL: $P = 0.013$–0.045; Heart-BackR: $P = 0.005$–0.041).

Cardio-muscular networks and reorganization across Exercise 1 and Exercise 2: residual fatigue. Cardio-muscular interactions between HR and muscle fibres of the leg and back muscles establish a multiplex network exhibiting significant heterogeneity. This network is distinguished by a unique topology and hierarchical organization specific to individual heart–muscle sub-networks in response to residual fatigue, as illustrated in Fig. 3*A*.

During Exercise 1, the link strength profiles for all heart–muscle sub-networks are characterized by stronger coupling between HR and low (F1–F5) EMG frequency bands compared with intermediate/high (F6–F10) EMG

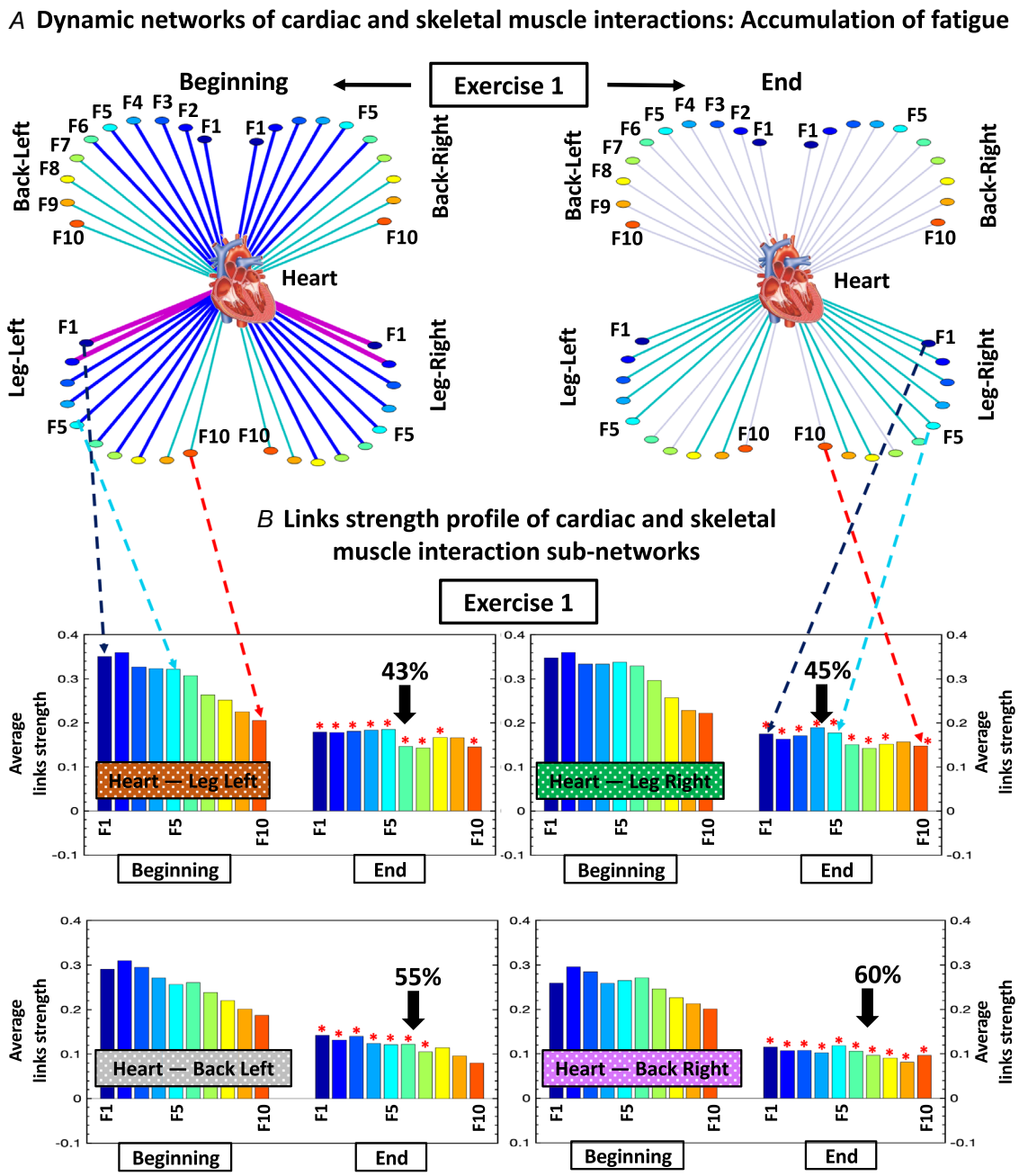

Figure 2. Dynamic network of cardiac and skeletal muscle interactions, and network reorganization with accumulation of fatigue
A, dynamic network of cardio-muscular interactions between instantaneous heart rate (HR) and major muscles involved in the squat movement. Group-averaged network map (n = 30), where network links represent the coupling strength (cross-correlation $C(HR,F_i)$) between HR and myoelectrical rhythms (frequency bands F_i) from Leg and Back muscles. Each heart–muscle sub-network contains 10 links quantifying the degree of synchronization (coupling) between HR and 10 muscle frequency bands F_i. Line width and colour indicate link strength (thicker/darker lines correspond to stronger coupling, Methods). Network maps derived from data corresponding to the Beginning (first third) and End (last third) segments of Exercise 1 show reorganization of the cardio-muscular network with accumulation of fatigue. Each muscle is represented as a semicircle with colour nodes for different frequency bands F_i (Methods). Cardio-muscular interactions between HR and muscle fibres from LegL/LegR and BackL/BackR muscles form a dynamic multiplex network with pronounced heterogeneity characterized by distinct topology and hierarchical organization of link strength. *B*, link strength profiles of cardio-muscular interaction sub-networks. Each of the 10 bars in the profile represents a link in the corresponding sub-network in (*A*), and

quantifies the coupling strength $C(HR,F_i)$ between HR and the EMG frequency bands F_i from a given muscle during Exercise 1. For the Beginning segment, the link strength profiles are characterized by stronger coupling between HR and the low F1–F5 EMG frequency bands (potentially corresponding to type I slow muscle fibres), compared with intermediate/high F6–F10 EMG bands (i.e. type II fast muscle fibres). With the accumulation of fatigue at the End of Exercise 1, a significant decline in coupling strength between HR and EMG frequency bands is observed for all sub-networks. Note that this decline is more pronounced for the coupling between HR and low-frequency (F1–F5) EMG bands, leading to a change in the link strength profiles – from a gradually declining profile at the Beginning to a flat profile at the End. Red stars mark statistically significant differences in link strength comparing Beginning with End (Wilcoxon's test P values <0.05). Note, P values are corrected for multiple comparisons using the Benjamini–Hochberg procedure for the 10 network links within each heart–muscle sub-network. The stronger coupling (and larger decline with fatigue) observed between HR and F1-F5 (type I slow muscle fibres) compared to F6-F10 (type II fast fibres), may be attributed to the distinctive aerobic/oxidative metabolism characteristic of type I fibres, contrasting with the anaerobic/glycolytic metabolism in type II fibres.

bands. Both Heart-Leg and Heart-Back sub-networks show similar link strength profiles. However, the Heart-Back sub-networks (bottom panels Fig. 3*B*) exhibit (i) weaker coupling and (ii) a more pronounced decrease across links from C(HR,F1) to C(HR,F10) within the profile compared with the Heart-Leg sub-networks (top panels Fig. 3*B*).

With residual fatigue during Exercise 2, a significant overall decline in coupling strength between HR and all EMG frequency bands is observed only for Leg muscles (Heart-Leg sub-networks; top panels Fig. 3*B*). Although the overall shape of the link strength profile is preserved with residual fatigue, there is a more pronounced decline in the coupling between HR and intermediate/high-frequency (F6–F10) EMG bands compared with the low-frequency (F1–F5) bands – note C values collapsing around zero. Red stars in Fig. 3*B* indicate statistically significant differences in link strength comparing Exercise 1 with Exercise 2 (Heart-LegL: $P = 0.0001$–0.019; Heart-LegR: $P = 0.0001$–0.001). The Heart-BackL and Heart-BackR sub-networks exhibit a minimal response to residual fatigue in Exercise 2 compared with Exercise 1 (Heart-BackL: $P = 0.931$–0.982; Heart-BackR: $P = 0.821$–0.994).

The results of the Fourier phase randomization surrogate test (see Methods) validate the physiological relevance of the derived cardio-muscular networks and their response to fatigue (Figs 2 and 3). After the Fourier phase randomization of the original EMG signals, the synchronous modulations in EMG frequency bands that capture the nonlinear features of EMG signals and contribute to effective cross-frequency coupling are removed. As a result, the cross-correlation C values between HR and the EMG frequency bands F_i from different muscles are significantly reduced for the surrogate data and collapse to $C \sim 0$. For Exercise 1, this surrogate test for all 10 links in the different sub-networks gives: Heart-LegL -0.0015 ± 0.007 (mean $\pm$ SD), Heart-LegR -0.0014 ± 0.007, Heart-BackL 0.009 ± 0.007 and Heart-BackR -0.0012 ± 0.006. For Exercise 2, the surrogate test for all 10 links in the different sub-networks gives: Heart-LegL sub-network -0.007 ± 0.01 (mean $\pm$ SD), Heart-LegR -0.0006 ± 0.01, Heart-BackL -0.009 ± 0.008 and Heart-BackR 0.0009 ± 0.008.

To assess the relative contribution of the periodic components and trends (Fig. 1) on the cross-correlation measures and derived cardio-muscular physiological networks shown in Fig. 3, we repeated our analysis after detrending the EMG frequency bands and HR signals but preserving the periodic patterns and their amplitude fluctuations (Fig. 4). Our findings indicate that removing linear trends, which reflect physiological response to sympato-vagal balance and fatigue, leads to an approximately 30% decline in the degree of cross-correlation (Fig. 4), compared with a 65% decline for non-detrended data (Fig. 3). These results demonstrate that trends account for approximately 50% of the observed decline in cardio-muscular coupling with fatigue (comparing network interactions during Exercise 1 *vs.* Exercise 2).

Finally, to provide more comprehensive details about the distribution and variability of the data obtained from different subjects presented in the link strength profiles in Fig. 3*B*, we displayed the median link strength and interquartile range (boxplots) for all sub-networks with residual fatigue for consecutive exercise bouts (Fig. 5).

Temporal variability in cardio-muscular coupling at short timescales

We further investigated the temporal coupling variability between HR and EMG spectral power frequency bands that occurred as a result of synchronous modulation of their amplitudes at short timescales of a few seconds (Fig. 6).

Figure 5 depicts cross-correlation moving averages for the Heart-LegL sub-network – C(HR,F1) and C(HR,F10) links – in 6 s windows with 3 s overlap (left panels), and corresponding normalized histograms of cross-correlation values (bottom blue/red and right panels), from two representative subjects. At the Beginning of Exercise 1, C values for the Heart-LegL sub-network are predominantly positive ($C > 0$; black) for both C(HR,F1) and C(HR,F10) links. In contrast,

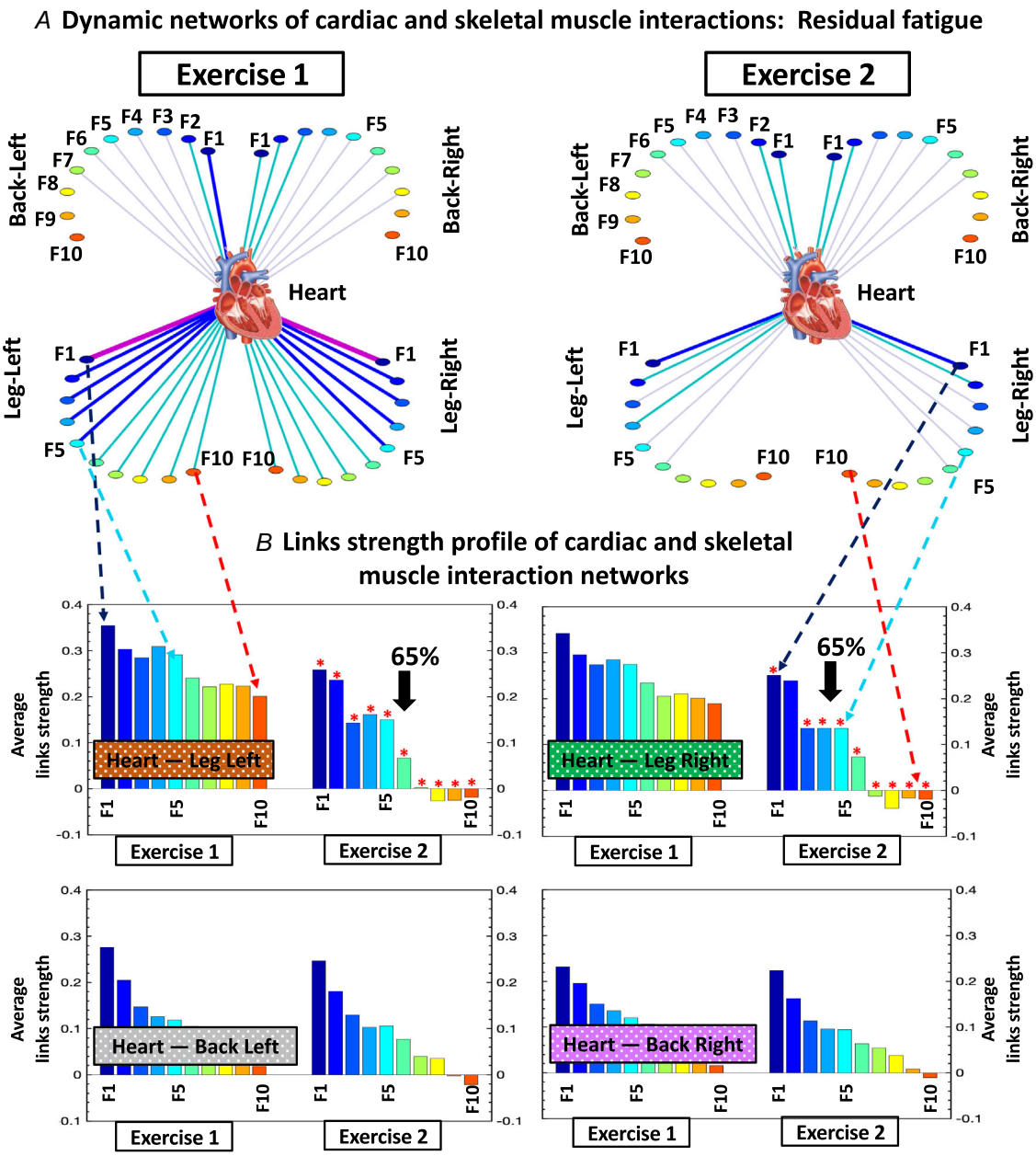

Figure 3. Dynamic network of cardiac and skeletal muscle interactions, and network reorganization with residual fatigue across exercise bouts
A, dynamic networks of cardio-muscular interactions between instantaneous heart rate (HR) and EMG frequency bands from Leg/Back muscles involved in the squat movement for consecutive Exercise 1 and Exercise 2 bouts. Shown are group-averaged network maps ($n = 30$), where network links represent the coupling (cross-correlation $C(HR,F_i)$) between HR and myoelectrical rhythms (frequency bands F_i) from Leg and Back muscles (Methods). Sub-networks in the cardio-muscular network contain 10 links that quantify the degree of synchronization (coupling) between HR and 10 bands F_i within a given muscle. Each muscle is represented as semicircle with colour nodes for different bands F_i. Line width and colour indicate network link strength (thicker/darker lines correspond to stronger coupling, Methods). Network maps derived from data during Exercise 1 and Exercise 2 show reorganization of topology and link strength with residual fatigue. *B*, link strength profiles of cardio-muscular interaction sub-networks for consecutive exercise bouts. Each of the 10 bars in the profile represents a link in the corresponding sub-network in (*A*), and quantifies the coupling strength $C(HR, F_i)$ between HR and the EMG frequency bands F_i from a given muscle. During Exercise 1, the link strength profiles are characterized by stronger coupling between HR and the low-frequency (F1–F5) EMG bands (potentially corresponding to type I slow muscle fibres), compared with intermediate/high-frequency (F6–F10) EMG bands (i.e. type II fast muscle fibres) for all sub-networks. For Exercise 2, a significant decline (∼65%) in coupling strength between HR and EMG

frequency bands is observed only for the Heart-Leg sub-networks. Note that this decline is more pronounced for the coupling between HR and the intermediate/high-frequency (F6–F10) EMG bands. Red stars mark statistically significant differences in link strength comparing Exercise 1 *vs*. Exercise 2 (Wilcoxon's test P values <0.05). Note, P values are corrected for multiple comparisons using the Benjamini–Hochberg procedure for the 10 network links within each heart–muscle sub-network. These changes in network organization and link strength profiles reflect residual fatigue during Exercise 2 and are notably different from the network reorganization associated with the accumulation of fatigue (Fig. 2). The differentiated response in link strength profiles of the Heart-Leg *vs*. Heart-Back sub-networks reflects the primary role of leg muscles compared with the supportive role of back muscles during squat movement, and to the different muscle fiber composition of these muscles.

at the End of Exercise 1 there is a dramatic transition to negative correlation values ($C < 0$; yellow) due to the accumulation of fatigue (Fig. 6 top panels). Notably, during Exercise 2, negative correlations are more present and occur from the Beginning of the bout because of residual fatigue provoked by Exercise 1. Notably, this effect is more pronounced for the coupling between HR and the F10 EMG frequency band C(HR,F10) compared with F1 EMG band C(HR,F1) in the LegL muscle – note the higher number of yellow C values for HR,F10 in Exercise 2. Accordingly, correlation distribution profiles reveal two classes of Heart-LegL coupling: stable positive correlations at the Beginning (predominantly $C > 0$; bottom blue histogram), and mixed correlations with accumulated fatigue at the End of Exercise 1 (bottom red histogram). The same effect is also observed comparing Exercise 1 with Exercise 2 (right brown histograms); where the distribution profile switches from homogeneity during Exercise 1 to heterogeneity during Exercise 2.

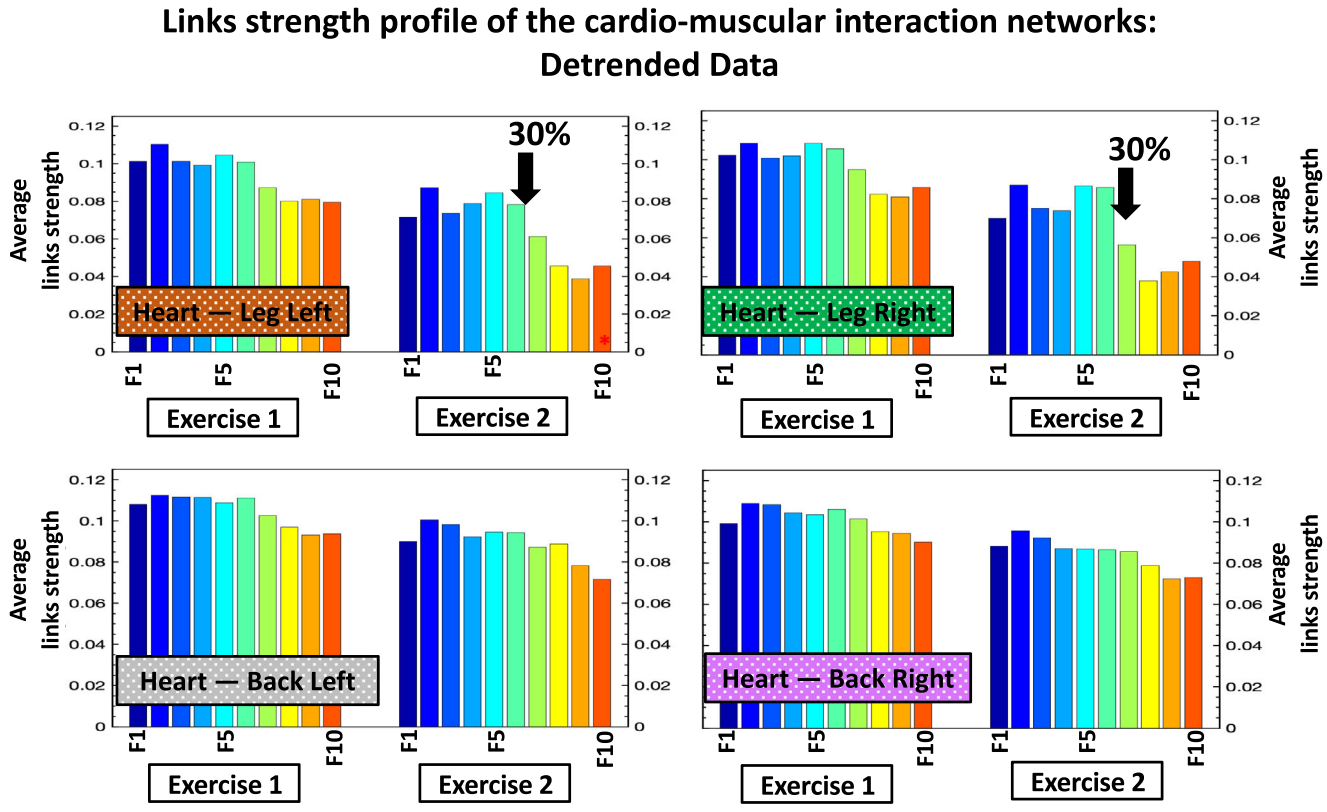

Figure 4. Link strength profiles of cardio-muscular interaction sub-networks for consecutive exercise bouts after data detrending
Each bar represents the coupling strength between heart rate (HR) and EMG frequency bands (cross-correlation $C(HR,F_i)$) from a given muscle, after linear detrending of the data. Notably, the structure of the cardio-muscular network profiles is similar in both the original results (Fig. 3) and the detrended data: stronger coupling between heart rate and lower EMG frequency bands compared with higher frequency bands (similar shape in the network link strength profile). However, linear detrending reduced the decline in coupling strength in Exercise 2 from ∼65% (without detrending: Fig. 3) to ∼30%, indicating that linear trends account for approximately 50% of the observed decline in cardio-muscular coupling with fatigue.

Cardio-muscular interaction profiles and degree of positive- and anti-correlation during Exercise 1: accumulation of fatigue. Since we observed complex transitions from synchronous to asynchronous behaviour with fatigue at short timescales of 3 s (Fig. 6), we next characterized the degree of positive- and anti-correlation between the heart and Leg/Back muscles (Fig. 7).

Figure 7*B* shows the group-average bar plots representing coupling strength derived from the cross-correlation distribution profiles for each heart–muscle sub-network at the Beginning and End of Exercise 1. For each pair of HR-EMG frequency band, bar height quantifies the probability of obtaining significant cross-correlation, where black positive bars represent the degree of positive correlation ($C > 0$), and yellow negative bars represent the degree of anti-correlation ($C < 0$; see Methods section *Global measures of cardio-muscular coupling at large timescales*). At the Beginning of Exercise 1 (Fig. 7*B* left panels), the strongest positive correlations occur between HR and low EMG frequency bands (F1–F4), while the strongest anti-correlations are observed between HR and high EMG bands (F8–F10). Note that both Heart-Leg and Heart-Back sub-networks show similar link strength profiles; however, coupling strength for the Heart-Back sub-networks is slightly weaker than for the Heart-Leg sub-networks.

With the accumulation of fatigue at the End of Exercise 1 (Fig. 7*B* right panels), the probability of positive correlations significantly decreases (∼20% across all links), while the probability of anti-correlations significantly increases (∼40% across all links). Red stars in Fig. 6*B* mark statistically significant differences in positive- (Heart-LegL: $P = 0.009$–0.023; Heart-LegR: $P = 0.0005$–0.008; Heart-BackL: $P = 0.022$–0.049; Heart-BackR: $P = 0.004$–0.021) and anti-correlation probabilities (Heart-LegL: $P = 0.007$–0.021; Heart-LegR: $P = 0.0006$–0.009; Heart-BackL: $P = 0.023$–0.043;

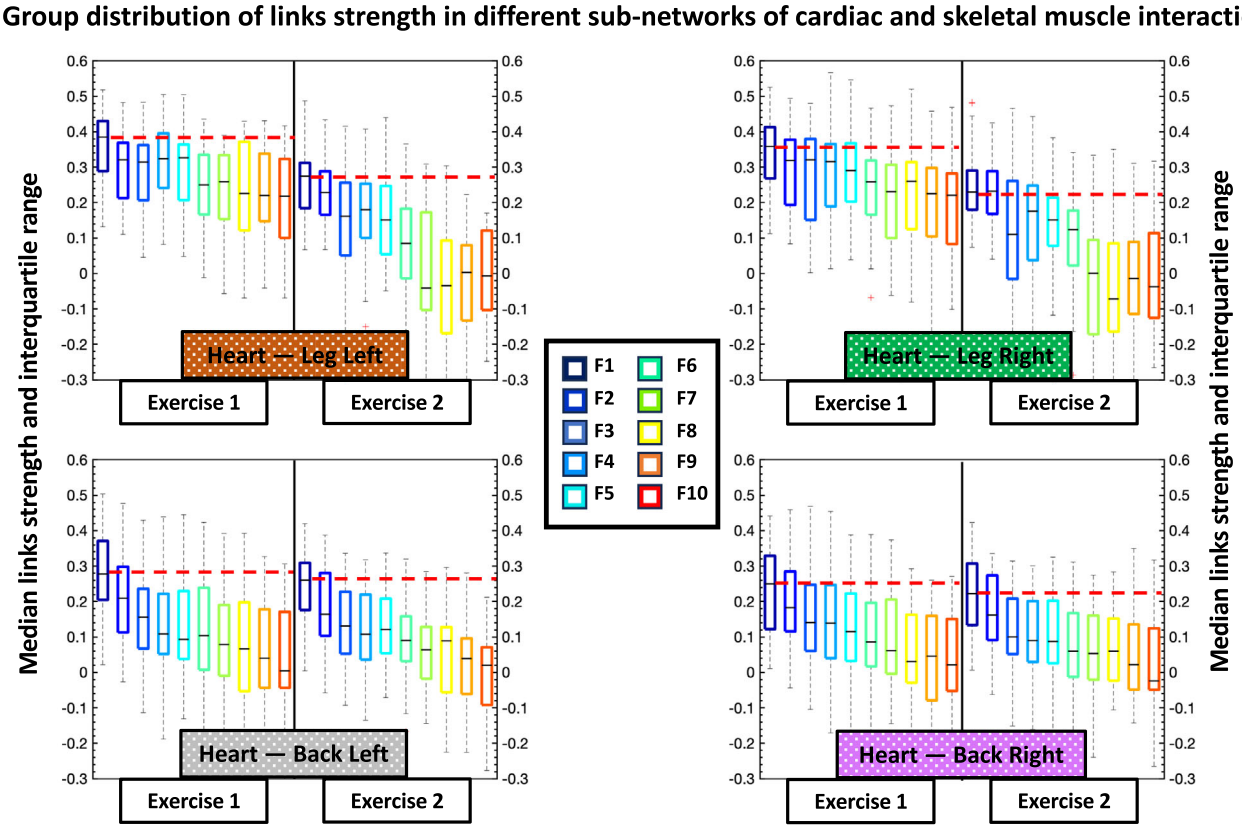

Figure 5. Group distribution of link strength in different sub-networks of cardiac and skeletal muscle interactions
Boxplots display the median link strength and interquartile range for different cardio-muscular sub-networks for the subjects in the database (different sub-network is shown in each panel; $n = 30$). Boxplots represent subject statistics for the average strength of each of the 10 links (shown in different box colours) in a given sub-network, comparing Exercise 1 with Exercise 2. Boxplots show inter-subject dispersity, correspond to the link strength stratification profiles in Fig. 3*B*, and reflect the effect of residual fatigue for Exercise 2. Data distribution supports the presence of characteristic link strength profiles that uniquely quantify each cardio-muscular sub-network and its response to fatigue.

Heart-BackR: $P = 0.005–0.027$) comparing Beginning with End of Exercise 1.

Figure 7C shows the group-averaged coexisting networks (i.e. visual representation) of positive- and anti-correlated interactions between HR and EMG bands F_i from Leg and Back muscles at the Beginning and End of Exercise 1. According to the bar plots in Fig. 7*B*, as fatigue accumulates at the End of Exercise 1, these two parallel networks undergo changes: positive-correlated networks weaken and anti-correlated networks strengthen significantly.

Cardio-muscular interaction profiles and degree of positive- and anti-correlation across Exercise 1 and Exercise 2: residual fatigue. During Exercise 1 (Fig. 8*A* left panels), the strongest positive correlations in the Heart-LegL and Heart-LegR sub-networks occur between HR and low EMG frequency bands (F1–F4), while the strongest anti-correlations are observed between HR and high EMG bands (F8–F10). With residual fatigue in Exercise 2 (Fig. 8*A* right panels), the probability of positive correlations in the Heart-LegL and Heart-LegR sub-networks significantly decreases (∼15% across all links), while the probability of anti-correlations significantly increases for all heart–muscle sub-networks (∼40% across all links). Note that the Heart-BackL and Heart-BackR sub-networks exhibit a less pronounced response to residual fatigue in Exercise 2 compared with Exercise 1. Red stars in Fig. 8*A* indicate statistically significant differences only for Heart-LegL and Heart-LegR sub-networks in positive- (Heart-LegL: $P = 0.035–0.045$; Heart-LegR: $P = 0.033–0.044$; Heart-BackL: $P = 0.164–0.195$; Heart-BackR: $P = 0.153$) and anti-correlation

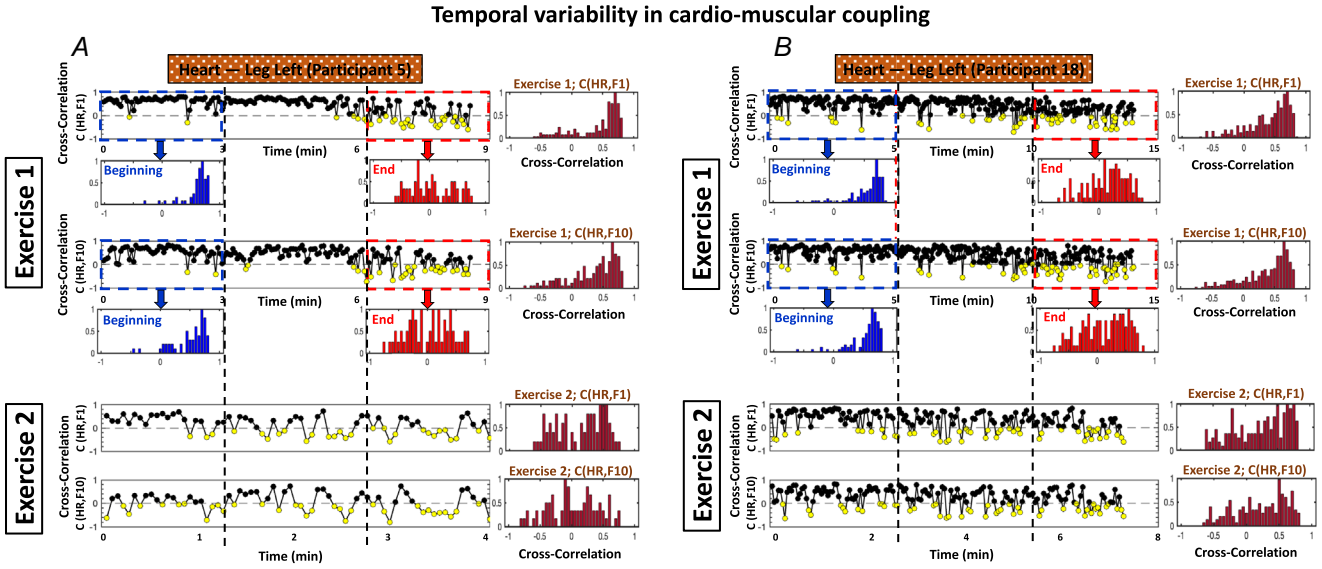

Figure 6. Temporal variability in cardio-muscular coupling during exercise
Time series of cross-correlation moving average values for two links in the Heart-LegL sub-network – *C*(HR,F1) and *C*(HR,F10) – obtained in 6 s windows with 3 s overlap (left panels), and the corresponding normalized histograms for Exercise 1 and Exercise 2 (right panels, brown for the entire exercise; bottom panels, blue and red for Beginning and End segments, respectively) from two representative subjects shown in (*A*) an (*B*). *C* values represent temporal cardio-muscular coupling in 3 s resolution and are predominantly positive (black) for both *C*(HR,F1) and *C*(HR,F10) links in the Beginning and Middle segments of Exercise 1. In contrast, the End segment of Exercise 1 shows a pronounced transition to higher variability with negative correlation values (yellow) due to the accumulation of fatigue. Note that during Exercise 2, negative cross-correlation *C* values are more prevalent compared with Exercise 1, and are also present during the Beginning and Middle segments of the bout due to residual fatigue provoked by Exercise 1. This effect is more pronounced for the *C*(HR,F10) coupling between HR and F10 EMG frequency band compared with the *C*(HR,F1) coupling of HR and F1 EMG band. The *C* value distribution reveals two classes of coupling: stable positive coupling at the Beginning (predominantly positive *C* values; bottom blue histogram), and mixed positive and negative coupling with the accumulation of fatigue at the End of Exercise 1 (bottom red histogram). For Exercise 2, due to residual fatigue, the *C* value distribution for all links (right panels, brown histograms) shows higher variability with almost equal probability for positive and negative coupling – in contrast to the predominantly positive coupling during Exercise 1. Distributions are rescaled by the peak *C* values of cross-correlation. The observed complex transitions from synchronous to asynchronous behaviour with both accumulation of fatigue and residual fatigue (consistently observed for all subjects in the database) highlight the relevance of examining the temporal variability of cardio-muscular coupling on a finer temporal scale for a comprehensive understanding of the mechanisms governing cardio-muscular network interactions.

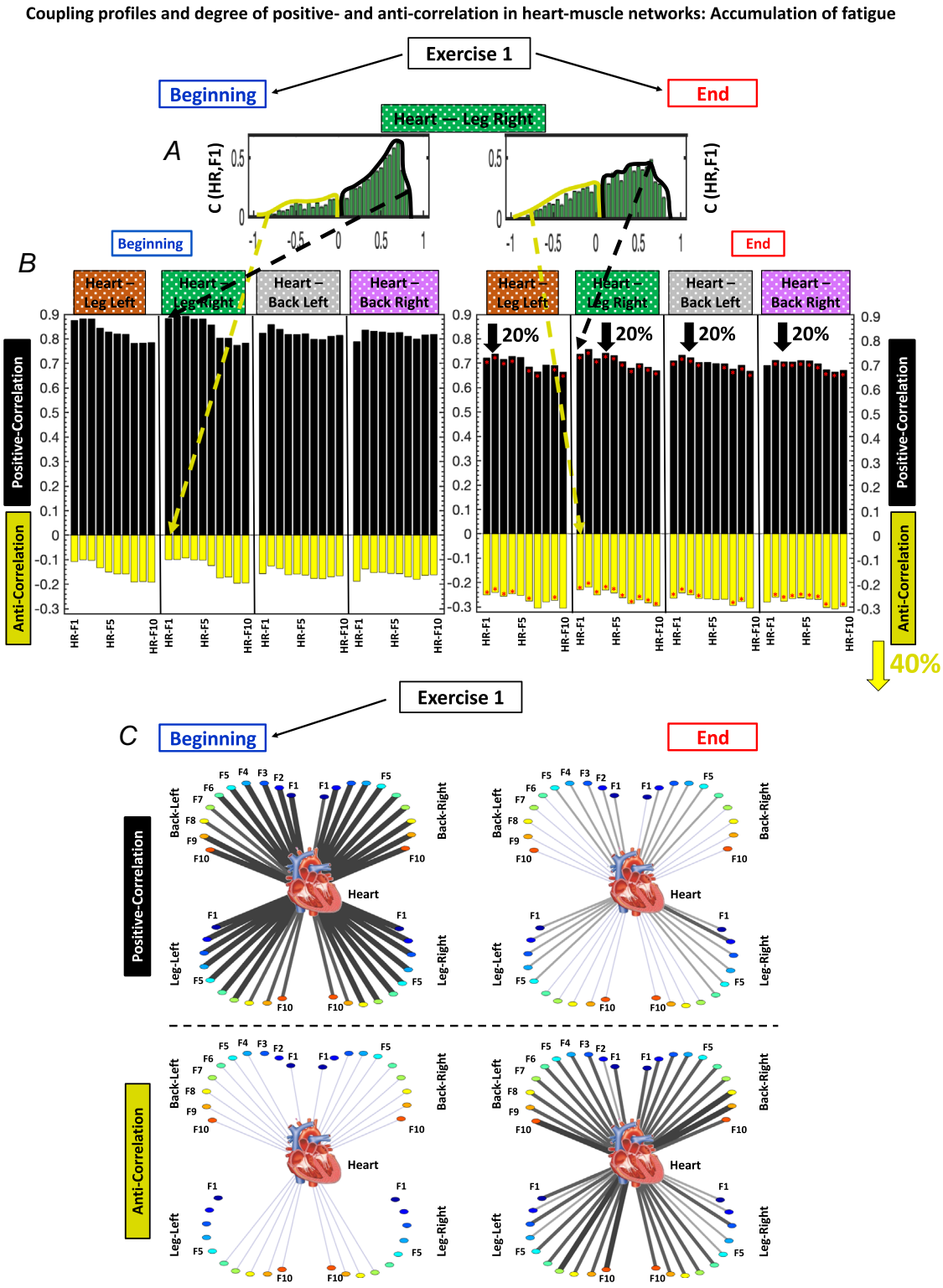

Figure 7. Coupling profiles, degree of positive- and anti-correlated interaction in cardio-muscular networks, and network reorganization with accumulation of fatigue
A, group-average distributions of cross-correlation values *C*(HR,F1) for the Heart-LegR sub-network for the Beginning (first third) and End (last third) segments of Exercise 1 (n = 30). Distribution histograms are rescaled by the peak *C* values of cross-correlation. The cross-correlation distribution profile significantly changes from the Beginning to the End of Exercise 1, indicating a transition with an accumulation of fatigue in the degree of positive (synchronous) and anti-correlated (asynchronous) coupling of heart rate (HR) and LegR frequency band F1 (in

agreement with coupling profiles for individual subjects, Fig. 6). *B*, group-averaged bar plots represent coupling strength derived from the cross-correlation distribution profiles for all pairs of HR and muscle frequency bands F_i in each cardio-muscular sub-network at the Beginning and End of Exercise 1. Bars quantify the probability of obtaining significant cross-correlation: positive bars (black) represent the degree of positive cross-correlation (area under distribution profile where $C > 0$), negative bars (yellow) represent the degree of anti-correlated coupling (area under distribution profile where $C < 0$; see Methods section *Fourier phase randomization surrogate test and significance threshold for link strength in networks of cardio-muscular interactions*). At the Beginning: the strongest positive coupling occurs between HR and low-frequency EMG bands (F1–F4) representing type I slow muscle fibres; and the strongest anti-correlated coupling is observed between HR and high-frequency EMG bands (F8–F10), which may represent type II fast muscle fibres. At the End, with accumulated fatigue: positive coupling significantly decreases (∼20%), while the anti-correlated coupling significantly increases (∼40%). This accumulated fatigue effect is observed for all cardio-muscular sub-networks. Red stars mark statistically significant differences in positive- and anti-correlated coupling comparing Beginning with End (Wilcoxon's test P values <0.05). Note, P values are corrected for multiple comparisons using the Benjamini–Hochberg procedure for the 10 network links within each heart–muscle sub-network. *C*, group-averaged cardio-muscular networks of positive- (top panels) and anti-correlated (bottom panels) interactions for the Beginning and End of Exercise 1, where network links correspond to the bars in (*B*). As fatigue accumulates at the End of Exercise 1, these parallel coexisting networks undergo a transition: links in the positive (synchronous) interactions network weaken; in contrast, links in the anti-correlated (asynchronous) interactions network become significantly stronger. The coexistence of synchronous and anti-synchronous behaviours represented by two parallel networks of positive- and anti-correlated interactions, demonstrates a complex duality and transient nature of cardio-muscular coupling that provides essential flexibility to dynamically adapt to accumulated fatigue.

probabilities (Heart-LegL: $P = 0.035$–0.045; Heart-LegR: $P = 0.034$–0.045; Heart-BackL: $P = 0.130$–0.171; Heart-BackR: $P = 0.164$–0.190) comparing Exercise 1 with Exercise 2.

Figure 8*B* depicts the group-averaged coexisting networks of positive- (top panels) and anti-correlated (bottom panels) interactions, between HR and myo-electrical rhythms (frequency bands F_i) from Leg and Back muscles in Exercise 1 and Exercise 2. With residual fatigue in Exercise 2, these coexisting networks undergo changes: positive-correlated networks weaken and anti-correlated networks strengthen significantly while maintaining network structure and organization (i.e. link strength profile).

Discussion

The present study investigated how autonomic regulation of cardiac function synchronizes with the activation of distinct muscles during a squat test performed until exhaustion, and established how the network of cardio-muscular interactions reorganizes with fatigue during consecutive exercise bouts. Uncovering how the heart coordinates its activation with distinct muscle fibre types is key to understanding the intricate mechanisms underlying autonomic cardiac regulation and skeletal muscle fibre activation, as well as global human function. In summary, (1) we identified profiles of cardio-muscular interactions with specific hierarchical organization of link strength; (2) these link strength profiles depend on the role muscles play during the squat movement (i.e. stronger coupling in Heart-Leg than in Heart-Back sub-networks), and on muscle fibre composition (i.e. stronger coupling between the heart and low EMG frequency bands representing type I slow muscle fibres); (3) the degree of cardio-muscular coupling decreases with fatigue, exhibiting a differentiated response for each sub-network; and (4) cardio-muscular profiles of link strength show similar characteristics and response to fatigue across timescales, featuring complex transitions from synchronous to asynchronous behaviour at short timescales of a few seconds.

Global cardio-muscular coupling at large timescales

At large timescales of observation, cardio-muscular interactions between instantaneous HR and EMG frequency bands from Leg and Back muscles form a multiplex network with pronounced heterogeneity, characterized by distinct topology and hierarchical organization for distinct heart–muscle sub-networks Figs (2*A* and 3*A*).

At the Beginning of Exercise 1 (Fig. 2), the link strength profiles for all heart–muscle sub-networks are characterized by stronger coupling between HR and low (F1–F5) EMG frequency bands compared with intermediate/fast (F6–F10) EMG bands. Since the average conduction velocity of an active motor unit relates to the muscle fibre type (Casolo et al., 2023), and changes in EMG spectral properties are linked to changes in the average conduction velocity of motor units (Farina, 2008; Von Tscharner & Nigg, 2008), the uncovered link strength profile in the heart–muscle sub-networks suggests that the heart may predominantly coordinate (synchronize activation) with slow type I fibres in the Leg and Back muscles. This stronger coupling observed between the heart and type I slow muscle fibres (F1–F5) compared with type II fast fibres (F6–F10), suggests a preference for coordinating with slow-twitch muscle fibres during the squat exercise. This coupling pattern aligns with

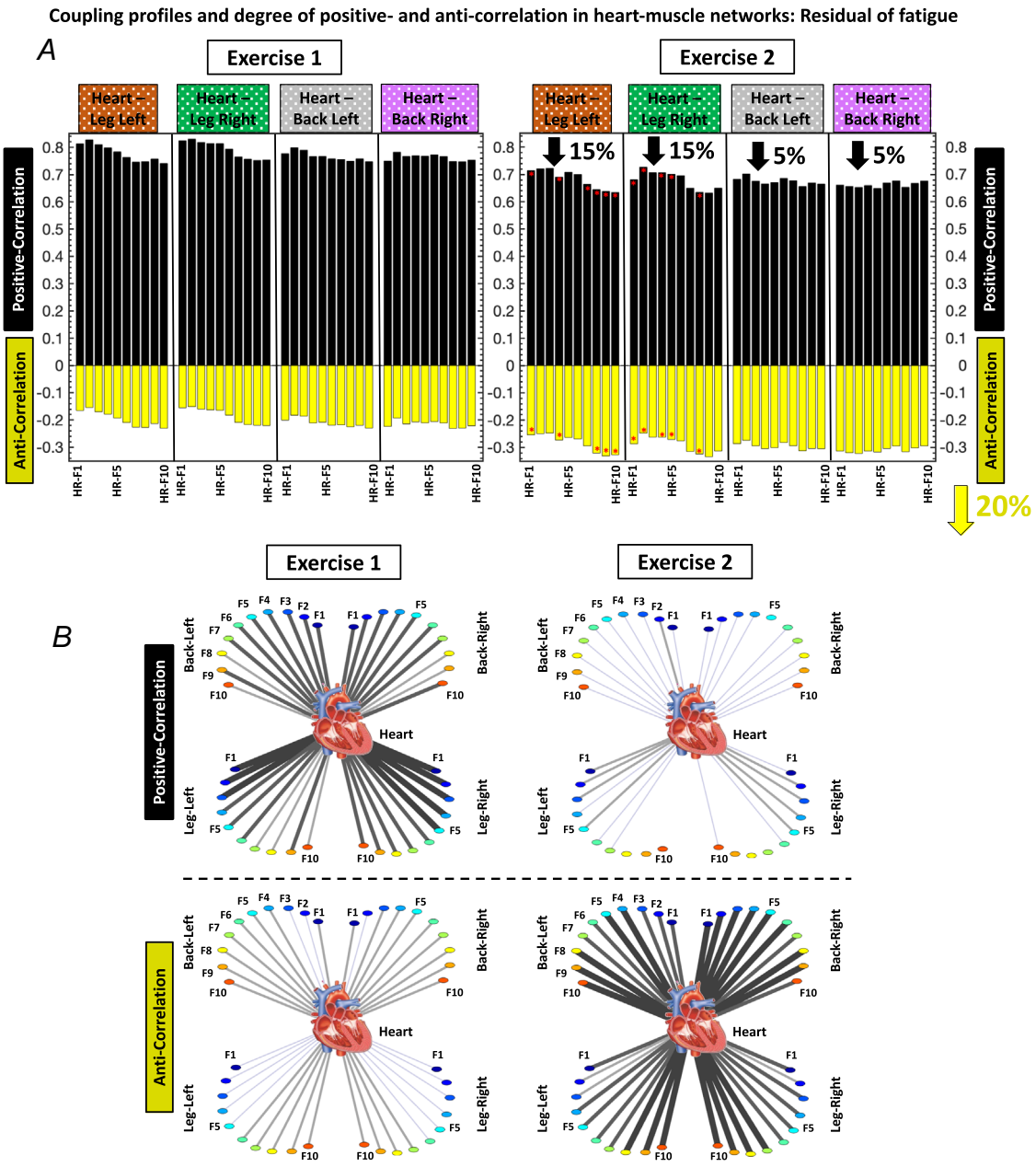

Figure 8. Degree of positive- and anti-correlated coupling in cardio-muscular networks with residual fatigue

A, group-averaged bar plots represent coupling strength derived from the cross-correlation distribution profiles for all pairs of heart rate (HR) and muscle frequency bands F_i in each cardio-muscular sub-network for consecutive Exercise 1 and Exercise 2 ($n = 30$). Positive bars (black) represent the degree of positive cross-correlation (area under distribution profile where $C > 0$), and negative bars (yellow) represent the degree of anti-correlated coupling (area under distribution profile where $C < 0$; see Methods section *Fourier phase randomization surrogate test and significance threshold for link strength in networks of cardio-muscular interactions*). For Exercise 1: the strongest positive coupling occurs between HR and low-frequency EMG bands (F1–F4) (less pronounced for the Heart-Back sub-networks); and the strongest anti-correlated coupling is observed between HR and high-frequency EMG bands (F8–F10). For Exercise 2, with residual fatigue: positive coupling significantly decreases (∼15%) for the Heart-Leg sub-networks, while the anti-correlated coupling significantly increases (∼40%) for all sub-networks. Red stars mark statistically significant differences in positive- and anti-correlated coupling comparing Exercise 1 with Exercise 2 (Wilcoxon's test P values <0.05). *B*, group-averaged cardio-muscular networks of positive- (top panels) and anti-correlated (bottom panels) interactions for Exercise 1 and Exercise 2, where network links correspond

to the bars in (*A*). These parallel coexisting networks undergo a transition with residual fatigue from Exercise 1 to Exercise 2: links in the positive (synchronous) interactions network weaken, while links in the anti-correlated (asynchronous) interactions network become significantly stronger during Exercise 2. The observed transition to dominant asynchronous coupling (negative cross-correlations) in cardio-muscular networks with fatigue (Figs. 7 and 8) can be attributed to specific physiological phenomena, including an autonomic shift towards sympathetic dominance, neuromuscular fatigue-induced changes in motor unit recruitment patterns, and the synchronization of cardiac and muscular dynamics.

the histochemical characteristics of muscle fibre types. Slow type I fibres, characterized by aerobic/oxidative metabolism and relying on oxygen for ATP (energy) production, are associated with a more sustained, endurance-oriented performance. This endurance capacity may become crucial during rhythmic activities like the squat movement. In contrast, fast type II fibres, which primarily utilize stored ATP, phosphocreatine and glycogen through glycolytic/anaerobic metabolism, are linked to more explosive and intense activities (Wackerhage, 2014). Additionally, while Heart-Leg (top panels Fig. 2*B*) and Heart-Back sub-networks (bottom panels Fig. 2*B*) show similar link strength profiles at the Beginning of Exercise 1, the coupling strength for the Heart-Back sub-networks is slightly weaker than for the Heart-Leg sub-networks. This observation may be related to the role selected muscles play during the squat movement – while vastus lateralis leg muscles have a primary motor role during squat movements, erector spinae back muscles have a secondary supportive role (trunk stability) (Garcia-Retortillo & Ivanov, 2022; Khaiyat & Norris, 2018). Remarkably, the findings reported for the Beginning of Exercise 1 (Fig. 2 left panels) are also present considering the entire bout of Exercise 1 (Fig. 3 left panels).

Importantly, with the accumulation of fatigue at the End of Exercise 1 (Fig. 2), a significant decline in coupling strength between HR and EMG frequency bands was observed for all heart–muscle sub-networks. This decline could be attributed to a multifaceted interplay of physiological factors. First, fatigue accumulation generates a progressive withdrawal of parasympathetic activity and the subsequent increase of sympathetic activity causing extensive changes in R–R intervals (Mongin et al., 2022). It is well established that the variability of HR decreases both in time and frequency according to several HRV indexes, including coarse graining spectral analysis (Borresen & Lambert, 2008), Poincaré plots (Tulppo et al., 1996) and HRV spectral power in different frequency bands (Arai et al., 1989; Cottin et al., 2004; Lewis et al., 2007). Second, fatigue induces changes in motor unit/muscle fibre recruitment with a notable shift towards lower frequencies in the EMG spectrum, due to reduced motor unit discharge rates and alterations in the shapes of motor unit action potentials (Beck et al., 2014). As shown in Fig. 1*D*, these changes led to (i) decreased variability and amplitude of HR time series, and (ii) increased amplitude and lower regularity of EMG spectral power time series. Consequently, these alterations could contribute to a reduction in the synchrony of oscillations between the two signals, as evidenced by lower correlation *C* values.

Alongside parasympathetic withdrawal and neuromuscular fatigue, it is crucial to consider the broader context of cardiovascular physiology to fully understand the decline in cardio-muscular coupling observed with fatigue at the End of Exercise 1. Standing up from a squat induces substantial phasic changes in systemic vascular resistance and venous return. Initially, the abrupt postural change causes gravitational pooling of blood in the lower extremities, leading to a transient reduction in venous return to the heart (Soloveva et al., 2020). This decrease in venous return momentarily lowers cardiac output and systemic blood pressure, which can compromise cerebral perfusion. The baroreceptors play a critical role in compensating for these haemodynamic changes, as they can detect the sudden drop in blood pressure and trigger a compensatory increase in HR and systemic vascular resistance to stabilize blood pressure and ensure adequate cerebral perfusion (Joyner, 2006; Ogoh & Ainslie, 2009). During exercise, the arterial baroreflex resets to regulate neural cardiovascular adjustments as exercise demands increase (Fadel & Raven, 2012). However, given the nature of the squat movement (i.e. constant changes in body position), the high levels of fatigue at the End of Exercise 1 could impact baroreflex capacity to sustain the necessary compensatory mechanisms of cerebral autoregulation to maintain constant perfusion. If baroreflex function is altered, there may be insufficient buffering of the sympathetic tone, causing augmented vasoconstriction and a greater increase in blood pressure, and decline in muscle blood flow (Crisafulli et al., 2015; Fadel & Raven, 2012; Fisher et al., 2008). This ultimately could lead to the pronounced reduction in cardio-muscular coupling (i.e. lower correlation *C* values) that we observed. Thus, integrating this broader view, the observed decline in cardio-muscular coupling and the End of Exercise 1 can be understood as a result of complex interactions among autonomic regulation, baroreceptor reflexes, venous return, motor unit recruitment and neuromuscular fatigue. This scenario is plausible since recent observations show synchronous adjustment of peripheral blood pressure and cerebral blood flow velocity within very short timescales of a single heartbeat (Chen et al., 2006).

The decline in cardio-muscular coupling strength with accumulated fatigue at the End of Exercise 1 (Fig. 2), is more pronounced for the coupling between HR and (F1–F5) EMG bands compared with (F6–F10) bands, leading to a change in the shape of the links strength profiles – from a profile with gradual decline in coupling strength at the Beginning, to a flat profile with similar coupling strength across all links at the End of Exercise 1 (Fig. 2*B*). The more pronounced decline in coupling strength for low (F1–F5) bands may be related to the Henneman principle, which states that motor units within a motor unit pool are recruited in an orderly manner, based on their excitability, from the smallest to the largest unit (Henneman et al., 1965). This means that slow type I, fatigue-resistant muscle fibres are activated before fast type II, less fatigue-resistant muscle fibres. As fatigue increases, more motor units need to be activated and recruited to maintain the same force output. Consequently, the more pronounced reduction in coupling strength primarily occurs in the slow type I muscle fibres (F1–F5) when comparing the Beginning with the End of Exercise 1, reflecting their predominant engagement during the initial segment of the bout.

With residual fatigue in Exercise 2 (Fig. 3), a significant decline in coupling strength between HR and all EMG frequency bands is also observed, but only for Heart-Leg sub-networks (top panels Fig. 3*B*). Although the overall shape of the link strength profile is preserved with residual fatigue, there is a more pronounced decline in the coupling between HR and intermediate/high-frequency (F6–F10) EMG bands compared with the low-frequency (F1–F5) bands, resulting in *C* values collapsing around zero. While type II fast fibres are active at the End of Exercise 1, their contribution may become minimal in Exercise 2 due to the fatigue generated by Exercise 1, highlighting their less fatigue-resistant nature.

Notably, the results of the Fourier phase randomization surrogate test (see Methods section Fourier phase randomization surrogate test) validate the physiological significance of the reported cardio-muscular networks. This test preserves the overall spectral power in the various frequency bands F_i within the EMG recordings while eliminating Fourier phase information related to nonlinear EMG characteristics and the associated modulation and heterogeneity in the EMG signals. After removing synchronous modulations in EMG frequency bands that contribute to effective cross-frequency coupling and capture the nonlinear features of EMG signals, the cross-correlation *C* values between HR and the EMG frequency bands F_i from different muscles were reduced and collapse around zero for the surrogate data. This indicates that the higher correlations observed in this study between HR and the EMG frequency bands F_i are largely due to nonlinear oscillations and synchronous modulations in the signals. The collapse of the cross-correlation *C* values after the Fourier phase randomization test suggests that these nonlinear characteristics are responsible for the apparent coupling, highlighting their significant role in cardio-muscular interactions.

Temporal variability in cardio-muscular coupling at short timescales

The temporal coupling variability between HR and EMG spectral power frequency bands that occur at short timescales of 3 s, is characterized by a complex transition from synchronous to asynchronous behaviour with fatigue (Fig. 6). Specifically, with the accumulation of fatigue at the End of Exercise 1 compared with the Beginning (Fig. 7), and with residual fatigue in Exercise 2 compared with Exercise 1 (Fig. 8), the probability of positive correlations ($C > 0$) significantly decreases while the probability for anti-correlations ($C < 0$) significantly increases. At the Beginning of Exercise 1, with low levels of fatigue, the HR oscillatory patterns match the 6 s periodicity in the EMG frequency bands (Fig. 1*D*). This reflects the effect of respiratory cycles on HR variability (RSA), where respiratory cycles are entrained with the tempo of squat movements. However, with the accumulation of fatigue at the End of Exercise 1, this synchronicity breaks down into asynchronous behaviour (i.e. dominance of negative correlations) as the breathing rate/frequency increases to satisfy the higher oxygen demands. This behaviour aligns with the classical empirical findings by Angelone & Coulter (1964) on how the RSA amplitude changes as a function of breathing frequency – changing the frequency of breathing results in a phase shift in the HR response relative to respiration. Specifically, as breathing rate increases due to fatigue, HR lags respiration and the phase angle between the two signals can even reach 180 degrees, indicating anti-phase at high breathing rates. This effect may explain why, in our results, we observed a transition towards a dominance of negative correlations ($C < 0$) between HR and EMG frequency bands at the End of Exercise 1, where the breathing rate is higher. However, we did not observe complete anti-phase correlations ($C \sim -1$) as the breathing rate of participants was not maximal due to the nature of the squat movement (maximal breathing rates >50 bm can be obtained during more global exercises such as high-intensity running).

Remarkably, at the Beginning of Exercise 1 (Fig. 7) as well as in the entire bout of Exercise 1, the strongest positive correlations occur between HR and low EMG (F1–F5) bands, while the strongest anti-correlations are observed between HR and high (F6–F10) bands. This finding aligns with the overall stronger coupling between HR and low (F1–F5) compared with high (F6–F10) bands

at larger timescales of observation (Figs 2 and 3). The stronger positive coupling observed between the heart and type I slow muscle fibres (F1–F5) suggests a preference for the heart to coordinate with slow-twitch muscle fibres during the squat exercise.

The coexistence of synchronous- and anti-synchronous behaviours represented by two parallel networks of positive- and anti-correlations (Figs 6*C* and 7*B*), demonstrates a complex duality and the transient nature of cardio-muscular coupling that provides essential flexibility to dynamically adapt to exercise-induced fatigue. This complex transition from synchronous to asynchronous behaviour highlights the relevance of examining the variability of cardio-muscular coupling on a finer temporal scale for a comprehensive understanding of the mechanisms governing cardiac and muscle function.

Notably, the findings at short timescales of a few seconds reported for the comparison Beginning *vs*. End of Exercise 1 with accumulation of fatigue (Fig. 7), are also evident in the comparison of Exercise 1 *vs*. Exercise 2 with residual fatigue (Fig. 8). Additionally, the results are consistent at several timescales of observation – long timescales (Figs 2 and 3) and short timescales of a few seconds (Figs 5–7). These findings reflect the presence of multiscale mechanisms underlying cardiovascular and muscular regulation of movements, and are in line with earlier studies that identified the presence of complex dynamics in the cardiovascular and muscular systems with invariant behaviour at different timescales (Ashkenazy et al., 2002; Hu et al., 2007; Ivanov et al., 2009; Karasik et al., 2002).

In view of the periodic oscillations embedded in both HRV and EMG spectral power data (Fig. 1*D*) induced by squat movements with controlled tempo (see Methods), we note that utilizing phase-synchronization analysis based on the Hilbert Transform would provide important information about the nature of cardio-muscular coupling and network interactions. Indeed, Hilbert Transform and phase-synchronization approaches have been successfully applied to quantify the dynamics and identify interactions of various physiological systems (Bartsch et al., 2012; Chen et al., 2006; Ivanov et al., 1996; Xu et al., 2006). However, measures of coupling based on phase-synchronization provide physiological information that is complementary and independent of amplitude–amplitude-based cross-correlation measures (Bartsch et al., 2014; Bartsch et al., 2015). Here, as the first step, we focussed on amplitude–amplitude cross-correlations that reflect changes with fatigue related to underlying periodic components and linear trends. In follow-up work, we will focus on phase-synchronization aspects in cardio-muscular coupling and network interactions.

The network physiology framework (Ivanov, 2021; Ivanov et al., 2016) employed in our study offers novel insights into the basic physiological mechanisms underlying cardio-muscular coordination. The work we present here expands on recent studies focusing on networks of cortico-muscular interactions (Rizzo et al., 2020; Rizzo et al., 2023). From a practical perspective, our approach holds promise for developing a new set of network-based markers capable of assessing and quantifying cardio-muscular interactions to assess global health, levels of fatigue, fitness status and the effectiveness of cardiovascular and muscle injury rehabilitation programmes. Establishing the baseline cardio-muscular networks can complement and overcome the limitations of traditional physiological parameters in assessing health and human function. Notably, gold standard physiological and performance variables (e.g. VO_{2max}, HR, power, etc.) provide little information on the nonlinear dynamic interactions among physiological systems, and cannot inform us about the qualitative synergetic reconfigurations that distinct physiological systems undertake to adjust the individual response to locomotion, exercise requirements and fatigue (Balagué et al., 2014, 2016; Garcia-Retortillo et al., 2019; Kerkman et al., 2022). Therefore, further research is warranted to (i) validate the universality of our findings across larger cohorts and define reference cardio-muscular network profiles for distinct movement patterns; (ii) explore the processes of reorganization and breakdown of cardio-muscular network interactions under various clinical conditions; and (iii) investigate the effects of distinct training/rehabilitation programmes on cardio-muscular coordination. Expanding research in these directions would establish the groundwork for a new interdisciplinary field of study: Network Physiology of Exercise (Balagué et al., 2020; Balagué, Garcia-Retortillo, et al., 2022; Balagué, Hristovski, et al., 2022).

In conclusion, (1) we uncovered the first profiles of cardio-muscular network interactions during exercise; (2) these profiles depend on the role muscles play during the squat movement (i.e. stronger coupling in Heart-Leg than in Heart-Back sub-networks), and on muscle fibre histochemical characteristics (i.e. stronger coupling between the heart and low EMG frequency bands representing type I slow muscle fibres); (3) the degree of cardio-muscular coupling decreases with fatigue due to parasympathetic withdrawal and neuromuscular fatigue; (4) cardio-muscular profiles of link strength show similar characteristics and response to fatigue across timescales, featuring complex transitions from synchronous to asynchronous behaviour at short timescales of a few seconds; and (5) the network approach we utilized introduces new avenues for the development of novel network-based markers, with the potential to characterize multilevel cardio-muscular and inter-muscular interactions.

References

Angelone, A., & Coulter, N.(1964). Respiratory a frequency sinus arrhythmia: A frequency dependent phenomenon. *Journal of Applied Psychology*, 479–482.

Arai, Y., Saul, J. P., Albrecht, P., Hartley, L. H., Lilly, L. S., Cohen, R. J., & Colucci, W. S.(1989). Modulation of cardiac autonomic activity during and immediately after exercise. *American Journal of Physiology*, **256**(1), 132–141.

Ashkenazy, Y., Hausdorff, J. M., Ch Ivanov, P.C,, & Eugene Stanley, H.(2002). A stochastic model of human gait dynamics. *Physica A*, **316**(1–4), 662–670.

Balagué, N., Aragonés, D., Hristovski, R., García, S., & Tenenbaum, G.(2014). Attention focus emerges spontaneously during progressive and maximal exercise. *Revista de Psicologia Del Deporte*, **23**(1), 57–63.

Balagué, N., Garcia-Retortillo, S., Hristovski, R., & Ivanov, P. C.(2022). From exercise physiology to network physiology of exercise. In R. Ferraz (Ed.), *Exercise physiology* (Vol., **11**, Issue tourism). https://doi.org/10.5772/intechopen.102756

Balagué, N., González, J., Javierre, C., Hristovski, R., Aragonés, D., Álamo, J., Niño, O., & Ventura, J. L.(2016). Cardio-respiratory coordination after training and detraining. A principal component analysis approach. *Frontiers in Physiology*, **7**, 35.

Balagué, N., Hristovski, R., Almarcha, M., Garcia-Retortillo, S., & Ivanov, P. C.(2020). Network physiology of exercise: Vision and perspectives. *Frontiers in Physiology*, **11**, 611550.

Balagué, N., Hristovski, R., Almarcha, M., Garcia-Retortillo, S., & Ivanov, P. C.(2022). Network physiology of exercise: Beyond molecular and omics perspectives. *Sports Medicine*, **8**(1), 119.

Bartsch, R. P. Liu, K. K. L., Bashan, A., & Ivanov, P. C.(2015). Network Physiology: How organ systems dynamically interact. *PLoS ONE*, **10**(11), e0142143.

Bartsch, R. P., Liu, K. K., Ma, Q. D., & Ivanov, P. C.(2014). Three independent forms of cardio-respiratory coupling: Transitions across sleep stages. *Computing in Cardiology*, **41**, 781–784.

Bartsch, R. P., Schumann, A. Y., Kantelhardt, J. W., Penzel, T., & Ivanov, P. C.(2012). Phase transitions in physiologic coupling. *Proceedings of the National Academy of Sciences*, **109**(26), 10181–10186.

Beck, T. W., Stock, M. S., & Defreitas, J. M.(2014). Shifts in EMG spectral power during fatiguing dynamic contractions. *Muscle & Nerve*, **50**(1), 95–102.

Bianco, A., Lupo, C., Alesi, M., Spina, S., Raccuglia, M., Thomas, E., Paoli, A., & Palma, A.(2015). The sit up test to exhaustion as a test for muscular endurance evaluation. *SpringerPlus*, **4**(1), 1–8.

Borresen, J., & Lambert, M. I.(2008). Autonomic control of heart rate during and after exercise measurements and implications for monitoring training status. *Sports Medicine (Auckland, N.Z.)*, **38**(8), 633–646.

Casolo, A., Maeo, S., Balshaw, T. G., Lanza, M. B., Martin, N. R. W., Nuccio, S., Moro, T., Paoli, A., Felici, F., Maffulli, N., Eskofier, B., Kinfe, T. M., Folland, J. P., Farina, D., & Vecchio, A. D.(2023). Non-invasive muscle biopsy: Estimation of muscle fibre size from a a neuromuscular interface. *The Journal of Physiology*, **601**(10), 1831–1850.

Chen, Z., Hu, K., Stanley, H. E., Novak, V., & Ivanov, P. C.(2006). Cross-correlation of instantaneous phase increments in pressure-flow fluctuations: Applications to cerebral autoregulation. *Physical Review E, Statistical, Nonlinear, and Soft Matter Physics*, **73**(3), 031915.

Christov, I. I.(2004). Real time electrocardiogram QRS detection using combined adaptive threshold. *BioMedical Engineering Online*, **3**(1). https://doi.org/10.1186/1475-925X-3–28

Constantini, K., Stickford, A. S. L., Bleich, J. L., Mannheimer, P. D., Levine, B. D., & Chapman, R. F.(2018). Synchronizing gait with cardiac cycle phase alters heart rate response during running. *Medicine and Science in Sports and Exercise*, **50**(5), 1046–1053.

Cottin, F, Médigue, C., Leprêtre, P. M., Papelier, Y., Koralsztein, J. P., & Billat, V. (2004). Heart rate variability during exercise performed below and above ventilatory threshold. *Medicine and Science in Sports and Exercise*, **36**(4), 594–600.

Crisafulli, A., Marongiu, E., & Ogoh, S.(2015). Cardiovascular reflexes activity and their interaction during exercise. *BioMed Research International*, **2015**, 1-10.

Dreibati, B., Lavet, C., Pinti, A., & Poumarat, G.(2010). Influence of electrical stimulation frequency on skeletal muscle force and fatigue. *Annals of Physical and Rehabilitation Medicine*, **53**(4), 266–277.

Fadel, P. J., & Raven, P. B.(2012). Human investigations into the arterial and cardiopulmonary baroreflexes during exercise. *Experimental Physiology*, **97**(1), 39–50.

Farina, D.(2008). Counterpoint: Spectral properties of the surface EMG do not provide information about motor unit recruitment and muscle fiber type. *Journal of Applied Physiology*, **105**(5), 1673–1674.

Faul, F., Erdfelder, E., Lang, A. G., & Buchner, A.(2007). G*Power 3: A flexible statistical power analysis program for the social, behavioral, and biomedical sciences. *Behavior Research Methods*, **39**(2), 175–191.

Fisher, J. P., Young, C. N., & Fadel, P. J.(2008). Effect of muscle metaboreflex activation on carotid-cardiac baroreflex function in humans. *American Journal of Physiology-Heart and Circulatory Physiology*, **294**(5), H2296-H2304.

Garcia-Retortillo, S., Gacto, M., O'Leary, T. J., Noon, M., Hristovski, R., Balagué, N., & Morris, M. G.(2019). Cardio-respiratory coordination reveals training-specific physiological adaptations. *European Journal of Applied Physiology*, **119**(8), 1701–1709.

Garcia-retortillo, S., & Ivanov, P. C.(2022). Inter-muscular networks of synchronous muscle fi ber activation. *Frontiers in Network Physiology*, **2**, 1059793.

Garcia-Retortillo, S., Javierre, C., Hristovski, R., Ventura, J. L., & Balagué, N.(2017). Cardiorespiratory coordination in repeated maximal exercise. *Frontiers in Physiology*, **8**, 387. https://doi.org/10.3389/FPHYS.2017.00387/BIBTEX

Garcia-Retortillo, S., Rizzo, R., Wang, J. W. J. L., Sitges, C., & Ivanov, P. C.(2020). Universal spectral profile and dynamic evolution of muscle activation: A hallmark of muscle type and physiological state. *Journal of Applied Physiology (Bethesda, Md: 1985)*, **129**(3), 419–441.

Garcia-Retortillo, S., Romero-Gómez, C., & Ivanov, P. C.(2023). Network of muscle fibers activation facilitates inter-muscular coordination, adapts to fatigue and reflects muscle function. *Communications Biology*, **6**(1), 891.

Garcia-Retortillo, S., Abenza, Ó., Vasileva, F., Balagué, N., Hristovski, R., Wells, A., Fanning, J., Kattula, J., & Ivanov, P. C. (2024). Age-related breakdown in networks of inter-muscular coordination. *GeroScience*. Advance online publication. https://doi.org/10.1007/s11357-024-01331-9

Grimby, L., Hannerz, J., & Hedman, B.(1979). Contraction time and voluntary discharge properties of individual short toe extensor motor units in man. *The Journal of Physiology*, **289**(1), 191–201.

Grimby, L., Hannerz, J., & Hedman, B.(1981). The fatigue and voluntary discharge properties of single motor units in man. *The Journal of Physiology*, **316**(1), 545–554.

Hader, K., Rumpf, M. C., Hertzog, M., Kilduff, L. P., Girard, O., & Silva, J. R.(2019). Monitoring the athlete match response: Can external load variables predict post-match acute and residual fatigue in soccer? A systematic review with meta-analysis. *Sports Medicine*, **5**(48). https://doi.org/10.1186/s40798-019–0219-7

Henneman, E., Somjen, G., & Carpenter, D. O.(1965). Excitability and inhibitility of motoneurons of different sizes. *Journal of Neurophysiology*, **28**(3), 599–620.

Hermens, H. J., Freriks, B., Disselhorst-Klug, C., & Rau, G.(2000). Development of recommendations for SEMG sensors and sensor placement procedures. *Journal of Electromyography and Kinesiology*, **10**(5), 361–374.

Hu, K., Scheer, J. L., Ivanov, P. C., Buijs, R. M., & Shea, S. A.(2007). The suprachiasmatic nucleus functions beyond circadian rhythm generation. *Neuroscience*, **149**(3), 508–517.

Ivanov, P. C.(2021). The new field of network physiology: Building the human physiolome. *Frontiers in Network Physiology*, **1**, 711778.

Ivanov, P. C., & Bartsch, R. P.(2014). Network Physiology: Mapping interactions between networks of physiologic networks. In *Networks of networks: The last frontier of complexity* (pp. 203–222). In G. D. Agostino & A. Scala (Eds.), Cham: Springer International Publishing.

Ivanov, P. C., Liu, K. K. L., & Bartsch, R. P.(2016). Focus on the emerging new fields of network physiology and network medicine. *In New Journal of Physics*, **18**(10), 100201.

Ivanov, P. C., Ma, Q. D. Y., Bartsch, R. P., Hausdorff, J. M., Nunes Amaral, L. A., Schulte-Frohlinde, V., Stanley, H. E., & Yoneyama, M.(2009). Levels of complexity in scale-invariant neural signals. *Physical Review E – Statistical, Nonlinear, and Soft Matter Physics*, **79**(4), 041920.

Ivanov, P. C, Amaral, L. A, Goldberger, A. L., & Stanley, H. E. (1998). Stochastic feedback and the regulation of biological rhythms. *Europhysics Letters*, **43**(4), 363–368.

Ivanov, P. C., Rosenblum, M. G., Peng, C. K., Mietus, J., Havlin, S., Stanley, H. E., & Goldberger, A. L.(1996). Scaling behaviour of heartbeat intervals obtained by wavelet-based time-series analysis. *Nature*, **383**(6598), 323–327.

Joyner, M. J.(2006). Baroreceptor function during exercise: Resetting the record. *Experimental Physiology*, **91**(1), 27–36.

Kantz, H., & Schreiber, T.(2003). *Nonlinear time series analysis*. Cambridge University Press.

Karasik, R., Sapir, N., Ashkenazy, Y., Ivanov, P. C., Dvir, I., Lavie, P., & Havlin, S.(2002). Correlation differences in heartbeat fluctuations during rest and exercise. *Physical Review E – Statistical, Nonlinear, and Soft Matter Physics*, **66**(6), 062902.

Kerkman, J. N., Zandvoort, C. S., Daffertshofer, A., & Dominici, N. (2022). Body weight control is a key element of motor control for toddlers' walking. *Frontiers in network physiology*, **2**, 844607.

Khaiyat, O. A., & Norris, J.(2018). Electromyographic activity of selected trunk, core, and thigh muscles in commonly used exercises for ACL rehabilitation. *Journal of Physical Therapy Science*, **30**(4), 642–648.

Kirby, R. L., Nugent, S. R., Marlow, R. W., MacLeod, D. A., & Marble, A. E.(1989). Coupling of cardiac and locomotor rhythms. *Journal of Applied Physiology*, **66**(1), 323–329.

Lewis, M. J., Kingsley, M., Short, A. L., & Simpson, K.(2007). Rate of reduction of heart rate variability during exercise as an index of physical work capacity. *Scandinavian Journal of Medicine & Science in Sports*, **17**(6), 696–702.

Lin, A., Liu, K. K. L., Bartsch, R. P., & Ch Ivanov, P.(2020). Dynamic network interactions among distinct brain rhythms as a hallmark of physiologic state and function. *Communications Biology*, **3**(1), 197.

Mccarthy, J. J., Gundersen, K., & Schwartz, L. M.(2019). Skeletal muscles do not undergo apoptosis during either atrophy or programmed cell death-revisiting the myonuclear domain hypothesis. *Frontiers in Physiology*, **9**(1887). https://doi.org/10.3389/fphys.2018.01887

Mongin, D., Chabert, C., Extremera, M. G., Hue, O., Courvoisier, D. S., Carpena, P., & Galvan, P. A. B.(2022). Decrease of heart rate variability during exercise: An index of cardiorespiratory fitness. *PLoS ONE*, **17**(9), 1–15.

Niizeki, K., Kawahara, K., & Miyamoto, Y.(1993). Interaction among cardiac, respiratory, and locomotor rhythms during cardiolocomotor synchronization. *Journal of Applied Physiology*, **75**(4), 1815–1821.

Nomura, K., Takei, Y., & Yanagida, Y.(2003). Comparison of cardio-locomotor synchronization during running and cycling. *European Journal of Applied Physiology*, **89**(3), 221–229.

O'rourke, M., Avolio, A., Stelliou, V., Young, J., & Gallagher, D. E.(1993). The rhythm of running: Can the heart join in? *Australian and New Zealand Journal of Medicine*, **23**(6), 708–710.

Ogoh, S., & Ainslie, P. N.(2009). Cerebral blood flow during exercise: Mechanisms of regulation. *Journal of Applied Physiology*, **107**(5), 1370–1380.

Pan, J., & Tompkins, W. J. (1985). A real-time QRS detection algorithm. *IEEE Transactions on Biomedical Engineering*, **32**(3), 230–236.

Peng, C. K., Havlin, S., Stanley, H. E., & Goldberger, A. L.(1995). Quantification of scaling exponents and crossover phenomena in nonstationary heartbeat time series. *Chaos (Woodbury, N.Y.)*, **5**(1), 82–87.

Phillips, B., & Jin, Y.(2013). Effect of adaptive paced cardio-locomotor synchronization during running: A preliminary study. *Journal of Sports Science and Medicine*, **12**, 381–387.

Podobnik, B., Fu, D. F., Stanley, H. E., & Ivanov, P. C.(2007). Power-law autocorrelated stochastic processes with long-range cross-correlations. *The European Physical Journal B*, **56**(1), 47–52.

Podobnik, B., Grosse, I., Horvatić, D., Ilic, S., Ivanov, P. C., & Stanley, H. E.(2009). Quantifying cross-correlations using local and global detrending approaches. *The European Physical Journal B*, **71**(2), 243–250.

Rabin, A., & Kozol, Z.(2017). Utility of the overhead squat and forward arm squat in screening for limited ankle dorsiflexion. *Journal of Strength and Conditioning Research*, **31**(5), 1251–1258.

Rizzo, R., Wang, J. W. J. L., Hohler, A. D., Holsapple, J. W., Vaou, O. E., & Ivanov, P. C.(2023). Dynamic networks of cortico-muscular interactions in sleep and neuro-degenerative disorders. *Forntiers in Network Physiology*, **3**, 1168677.

Rizzo, R., Zhang, X., Wang, J. W. J. L., Lombardi, F., & Ivanov, P. C.(2020). Network physiology of cortico-muscular interactions. *Frontiers in Physiology*, **11**, 558070.

Rosenblum, U., Melzer, I., Zeilig, G., & Plotnik, M.(2021). Muscle activation profile during perturbed walking is modulated according to body state. *bioRxiv*, **6**. https://doi.org/10.1101/2021.01.13.426393

Schreiber, T., & Schmitz, A.(2000). Surrogate time series. *Physica D: Nonlinear Phenomena*, **142**(3–4), 346–382.

Sieciński, S., Kostka, P. S., & Tkacz, E. J.(2020). Heart rate variability analysis on electrocardiograms, seismocardiograms and gyrocardiograms on healthy volunteers. *Sensors*, **20**(4522). https://doi.org/10.3390/s20164522

Soloveva, A., Fedorova, D., Villevalde, S., Zvartau, N., Mareev, Y., Sitnikova, M., Shlyakhto, E., & Fudim, M.(2020). Addressing orthostatic hypotension in heart failure: Pathophysiology, clinical implications and perspectives. *Journal of Cardiovascular Translational Research*, **13**(4), 549–569.

Theiler, J., Eubank, S., Longtin, A., Galdrikian, B., & Doyne Farmer, J.(1992). Testing for nonlinearity in time series: The method of surrogate data. *Physica D: Nonlinear Phenomena*, **58**(1–4), 77–94.

Tulppo, M. P., Mäkikallio, T. H., Takala, T. E. S., Seppänen, T., & Huikuri, H. V.(1996). Quantitative beat-to-beat analysis of heart rate dynamics during exercise. *American Journal of Physiology*, **271**(1), 244–252.

Vázquez, P., Hristovski, R., & Balagué, N.(2016). The path to exhaustion: Time-variability properties of coordinative variables during continuous exercise. *Frontiers in Physiology*, **7**, 37.

Vigotsky, A. D., Halperin, I., Lehman, G. J., Trajano, G. S., & Vieira, T. M.(2018). Interpreting signal amplitudes in surface electromyography studies in sport and rehabilitation sciences. *Frontiers in Physiology*, **8**(985). https://doi.org/10.3389/fphys.2017.00985

Von Tscharner, V., & Nigg, B. M.(2008). Counterpoint: Spectral properties of the surface EMG can characterize/do not provide information about motor unit recruitment strategies and muscle fiber type. *Journal of Applied Physiology*, **105**(5), 1671–1673.

Wackerhage, H.(2014). Molecular exercise physiology: An introduction. In *Molecular exercise physiology: An introduction*. Routledge. https://doi.org/10.4324/9780203132142

Wakeham, D. J., Ivey, E., Saland, S. A., Lewis, J. S., Palmer, D., Morris, M., Bleich, J. L., Weyand, P. G., Brazile, T. L., Hearon, C. M., Sarma, S., MacNamara, J. P., Hieda, M., & Levine, B. D.(2023). Effects of synchronizing foot strike and cardiac phase on exercise hemodynamics in patients with cardiac resynchronization therapy: A within-subjects pilot study to fine-tune cardio-locomotor coupling for heart failure. *Circulation*, **148**(25), 2008–2016.

Wakeling, J. M., Pascual, S. A., Nigg, B. M., & Tscharner, V.(2001). Surface EMG shows distinct populations of muscle activity when measured during sustained sub-maximal exercise. *European Journal of Applied Physiology*, **86**(1), 40–47.

Walløe, L., & Wesche, J.(1988). Time course and magnitude of blood flow changes in the human quadriceps muscles during and following rhythmic exercise. *The Journal of Physiology*, **405**(1), 257–273.

Xu, L., Chen, Z., Hu, K., Stanley, H. E., & Ivanov, P. C.(2006). Spurious detection of phase synchronization in coupled nonlinear oscillators. *Physical Review E—Statistical, Nonlinear, and Soft Matter Physics*, **73**(6), 065201.

Yavuz, H. U., Erdağ, D., Amca, A. M., & Aritan, S.(2015). Kinematic and EMG activities during front and back squat variations in maximum loads. *Journal of Sports Sciences*, **33**(10), 1058–1066.

Additional information

Data availability statement

All data supporting the findings of the present study are presented in the article. However, any additional data are available upon reasonable request from the corresponding author.

Competing interests

None declared.

Author contributions

P.C.I. and S.G.R. conceived the idea and designed the study. S.G.R. and P.C.I. designed the experimental protocol and collected data. S.G.R. performed data pre-processing and developed codes for the analysis method. S.G.R. and P.C.I. performed data analyses and prepared the figures. S.G.R. and P.C.I. performed surrogate and statistical tests, performed research and interpreted results. S.G.R. and P.C.I. wrote the manuscript, read and approved the submitted version. All authors have approved the final version of the manuscript and

agree to be accountable for all aspects of the work. All persons designated as authors qualify for authorship, and all those who qualify for authorship are listed.

Funding

The authors acknowledge support from the W. M. Keck Foundation, the US-Israel Binational Science Foundation (BSF Grant 2 020 020) and the Translational Research Centre (Wake Forest University; ID0576−590 006-U05244).

Acknowledgements

We thank Dr Hugo Posada-Quintero for his assistance with EKG data processing, Maddie Sayre and Maddie Davis for their help with data collection and participant recruitment, and Óscar Abenza Ortega for his assistance in revising the final version of the manuscript. We also thank Dr Peter H. Brubaker for his insightful discussion and help in providing physiological interpretation of the results.

Keywords

cardiac electrophysiology, cardio-muscular coordination, complex systems, dynamic networks, electromyography, fatigue, heart rate variability, muscle fibres, network physiology, synchronization

Supporting information

Additional supporting information can be found online in the Supporting Information section at the end of the HTML view of the article. Supporting information files available:

Peer Review History